NATIONAL ADVISORY COMMITTEE FOR AERONAUTICS

TECHNICAL NOTE 3644

LIFT AND MOMENT COEFFICIENTS FOR AN OSCILLATING RECTANGULAR WING-AILERON CONFIGURATION IN SUPERSONIC FLOW

By Julian H. Berman

Langley Aeronautical Laboratory
Langley Field, Va.

Washington
July 1956

NATIONAL ADVISORY COMMITTEE FOR AERONAUTICS

TECHNICAL NOTE 3644

LIFT AND MOMENT COEFFICIENTS FOR AN OSCILLATING RECTANGULAR WING-AILERON CONFIGURATION IN SUPERSONIC FLOW

By Julian H. Berman

SUMMARY

Linearized theory for compressible unsteady flow is used to treat the problem of a partial-span rectangular control surface, hinged at its leading edge and mounted on a rectangular wing, oscillating in supersonic flow. The motions of the wing-aileron configuration are assumed to consist of vertical translation, pitching, and aileron rotation. The velocity potentials for this configuration are derived as power series in terms of a frequency parameter to the fifth power of the frequency of oscillation. From these potentials closed expressions for section force and moment coefficients at any spanwise location are derived. The section force and moment coefficients are employed in a particular flutter study in which the spanwise position of the aileron is varied.

INTRODUCTION

The problem of the oscillating rectangular wing in supersonic flow has been investigated in several papers (refs. 1 to 4). In reference 1 the velocity potential was derived as a power series in terms of a frequency parameter for vertical translation and pitching oscillations, and expressions for the aerodynamic derivatives to the third power of the frequency were presented. The aerodynamic derivatives obtained in reference 2 were presented in the form of double integrals. Reference 3, employing the Laplace transform, presented the disturbance velocity potential as a definite integral. This last result was used in reference 4 to derive the complete series expansion in terms of frequency for the disturbance velocity potential from which aerodynamic derivatives of the kind given in reference 1 were obtained to the seventh power of the frequency.

The problem of a rectangular control surface mounted on a rectangular wing, which is a logical extension of the wing problem, is the subject of the present paper. This configuration (herein designated as a rectangular "wing-aileron") has been considered for steady flow in a number of papers, for example, reference 5. The unsteady-flow problem was considered in reference 6 for a control surface hinged at its leading edge, with the outboard edge at the wing tip and the gap between it and the wing at the inboard edge assumed to be sealed. The results of reference 6, expressions for forces and moments on spanwise strips, are presented in the form of double integrals. A later paper, reference 7, applied these results to obtain expressions for total aerodynamic derivatives for a wing-aileron combination.

In the forms presented the results of references 6 and 7 are not particularly useful in flutter analyses employing beam theory, since this type of analysis calls for spanwise distributions of air forces and moments. In the present paper the configuration of reference 6 is considered and, by extending the methods of references 1 and 4 to include a control surface, the expressions are obtained for the section lift and moment coefficients at any spanwise station of the wing-aileron configuration from power-series expansions of the velocity potential in terms of a frequency parameter. The expressions presented include terms to the fifth power of the frequency of oscillation. To gain some insight into the overall effect of aspect ratio upon the forces and moments, expressions are also given for the total forces and moments of the wing-aileron combination.

The spanwise variation of the lift and moment coefficients developed in the present paper are shown for a set of conditions. The section force and moment coefficients are applied for a single Mach number to illustrate the flutter characteristics of some configurations having partial-span ailerons for three degrees of freedom. A comparison is provided with similar calculations involving two degrees of freedom.

SYMBOLS

A	aspect ratio of wing
b	semichord of wing
c	speed of sound in undisturbed medium

$$F_n(x,y) = \int_0^x x^{n-1}\sin^{-1}\sqrt{\frac{\beta y}{x}}\,dx$$

$$F_n'' = \int_0^{x_1} x^{n-1}\sin^{-1}\sqrt{\frac{\beta y}{x}}\,dx$$

$$F_n''' = \int_0^{x_3} x^{n-1} \sin^{-1}\sqrt{\frac{\beta y}{x}}\, dx$$

$\bar{\bar{F}}_n = F_n(1,y)$

h vertical displacement of axis of rotation, positive downward

$\dot{h},\dot{\alpha},\dot{\delta}$ time derivatives of h, α, and δ, respectively

I_α moment of inertia of wing-aileron combination about elastic axis per unit span length

I_β moment of inertia of aileron about x_1 (hinge axis) per unit span length

$J_0(\ )$ Bessel function of zero order (first kind)

k reduced frequency, $b\omega/V$

L_i,M_i,N_i components of section force and moment coefficients ($i = 1, 2, \ldots 6$ as defined in eq. (26))

$\bar{L}_i,\bar{M}_i,\bar{N}_i$ components of total force and moment coefficients ($i = 1, 2, \ldots 6$ as defined in eq. (33))

m mass of wing-aileron combination per unit span length

M Mach number, V/c

M_α aerodynamic section moment on wing about wing axis of rotation, positive leading edge up

$\bar{M}_\alpha$ total aerodynamic moment on wing about wing axis of rotation, positive leading edge up

M_δ aerodynamic section moment on aileron about its hinge, positive leading edge up

$\bar{M}_\delta$ total aerodynamic moment on aileron about its hinge, positive leading edge up

Δp local pressure difference between upper and lower surfaces, positive downward

P	aerodynamic section normal force, positive downward
$\bar{P}$	total aerodynamic force on wing, positive downward
r_α	radius of gyration of wing-aileron combination referred to x_o; $\sqrt{I_\alpha/mb^2}$
r_β	reduced radius of gyration of aileron referred to x_1; $\sqrt{I_\beta/mb^2}$
S_β	static moment of aileron per unit span length referred to x_1
t	time
V	flight velocity
w	vertical velocity at surface of wing
x,y,z	rectangular coordinates attached to wing moving in negative x-direction
x_o	coordinate of wing axis of rotation
x_1	coordinate of aileron hinge

$x_2 = x - x_1$

$x_3 = 1 - x_1$

x_α	location of center of gravity of wing-aileron combination referred to x_o
x_β	reduced location of center of gravity of aileron referred to x_1; S_β/mb
y_1	spanwise location of inboard aileron tip
α	angular displacement of wing about wing axis of rotation, positive leading edge up

$\beta = \sqrt{M^2 - 1}$

δ angular displacement of aileron, measured relative to α, positive trailing edge down

$\kappa = \pi\rho b^2/m$

ρ density of the medium

ϕ disturbance velocity potential

ϕ_δ subsidiary velocity potential associated with aileron position

$\phi_{\dot{\delta}}$ subsidiary velocity potential associated with aileron motion

ω circular frequency of oscillation

$\bar{\omega} = M^2\omega/V\beta^2$

ω_h first natural bending frequency of wing

ω_α first natural torsion frequency of wing

ω_δ natural rotational frequency of aileron

ANALYSIS

Outline of Problem

Consider a thin, flat, rectangular wing-aileron configuration moving at a constant supersonic velocity V, as shown in figure 1. The Mach lines emanating from the foremost points of the wing and aileron tips divide the configuration into various regions. The potentials for the various regions of the wing delineated by the Mach lines from the wing-leading-edge tips have been derived and discussed in several papers (refs. 1 to 4). This paper will deal with the potentials for the various regions delineated by the Mach lines from the aileron leading-edge tips. A restrictive condition for the present treatment, similar to that employed for the treatment of the rectangular wing in reference 1, is that the Mach line from the foremost point of one aileron tip does not intersect the opposite tip ahead of the trailing edge.

A rectangular coordinate system x,y,z, moving uniformly with the wing in the negative x-direction, is adopted so that the xy-plane is coincident with the mean position of the wing, and the origin is taken at the intersection of the wing leading edge and the wing tip. The outboard edge of the aileron is coincident with the wing tip ($y = 0$), and the inboard edge ($y = y_1$) adjoins the wing proper. (This same configuration is treated in ref. 6.) The aileron is hinged at its leading edge, and the gap at its inboard edge is assumed to be sealed.

The wing-aileron combination is considered to be performing the following types of small-amplitude harmonic oscillations with frequency ω: vertical translation h and pitching α about a spanwise axis x_o. In addition the aileron is allowed to perform a rotational oscillation about a spanwise axis x_1. The vertical displacement at any chordwise point x of the wing-aileron is therefore

$$z = h + \alpha(x - x_o) + \delta(x - x_1) \tag{1}$$

where the δ term vanishes for $x < x_1$ or $y > y_1$. The normal velocity at any point of the wing-aileron may then be expressed as

$$w = \dot{h} + V\alpha + \dot{\alpha}(x - x_o) + V\delta + \dot{\delta}(x - x_1) \tag{2}$$

The velocity potential for the wing-aileron configuration may be expressed as the sum of separate effects due to position and velocity of the configuration associated with the individual terms in equation (2) as

$$\phi = \phi_{\dot{h}} + \phi_{\alpha} + \phi_{\dot{\alpha}} + \phi_{\delta} + \phi_{\dot{\delta}} \tag{3}$$

The first three terms on the right side of equation (3) apply to purely wing oscillations and were treated in power-series form in reference 1 to the third power of the frequency and in reference 4 to the seventh power. The last two terms on the right side apply to control-surface oscillations and will be treated in the following section.

Aileron Velocity Potentials

Consider the flow field of the aileron, for which ϕ_{δ} and $\phi_{\dot{\delta}}$ are the velocity potentials. The field is divided into three regions (fig. 1): region I behind the outboard Mach line, region III within the inboard Mach cone, and region II which is the remaining part of the control surface. Expressions for the velocity potential in these various regions will now be obtained.

Regions I and II.- In accordance with linearized theory the velocity potential for regions I and II can be obtained directly from the velocity potential of a semi-infinite rectangular wing. This is because the aileron is not affected by the presence of the wing when the wing is at constant zero angle of attack and is therefore essentially a wing itself. The boundary-value problem for the semi-infinite rectangular wing was solved by means of the Laplace transform in reference 3. The transform of the velocity potential was obtained in the form

$$(\bar{\phi})_{z=0} = -\frac{\bar{w}}{\beta}\left(\frac{1}{\mu} - \frac{2}{\pi\mu}\int_0^{\pi/2} e^{-\mu y \sec^2\theta}\, d\theta\right) \tag{4}$$

where

$$\mu = \sqrt{\bar{x}^2\beta^2 + 2M\bar{x}\frac{i\omega}{c} - \frac{\omega^2}{c^2}}$$

$$\beta = \sqrt{M^2 - 1}$$

and where the bar above w, ϕ, and x denotes the Laplace transformation of these terms with respect to x.

Employing the δ and $\dot{\delta}$ components of equation (2) in equation (4) and applying the inverse Laplace transform (pairs 55 and 84, pp. 298-299, ref. 8) result in the following expressions for the aileron potentials ϕ_δ and $\phi_{\dot{\delta}}$ in regions I and II:

$$\phi_\delta = -\frac{V\delta}{\beta}\int_0^{x-x_1}\left[J_0\left(\frac{\bar{\omega}x}{M}\right) - \frac{2}{\pi}\int_0^{\sec^{-1}\sqrt{\frac{x}{\beta y}}} J_0\left(\frac{\bar{\omega}}{M}\sqrt{x^2 - \beta^2y^2\sec^4\theta}\right)d\theta\right]e^{-i\bar{\omega}x}dx \tag{5}$$

$$\phi_{\dot{\delta}} = -\frac{\dot{\delta}}{\beta}\int_0^{x-x_1}\int_0^x\left[J_0\left(\frac{\bar{\omega}x}{M}\right) - \frac{2}{\pi}\int_0^{\sec^{-1}\sqrt{\frac{x}{\beta y}}} J_0\left(\frac{\bar{\omega}}{M}\sqrt{x^2 - \beta^2y^2\sec^4\theta}\right)d\theta\right]e^{-i\bar{\omega}x}(dx)^2$$

$$= -\frac{\dot{\delta}}{\beta}\left[(x - x_1)\int_0^{x-x_1} J_0\left(\frac{\bar{\omega}x}{M}\right)e^{-i\bar{\omega}x}\,dx - \int_0^{x-x_1} xJ_0\left(\frac{\bar{\omega}x}{M}\right)e^{-i\bar{\omega}x}\,dx - \right.$$

$$\left.\frac{2}{\pi}\int_0^{x-x_1}\int_0^x\int_0^{\sec^{-1}\sqrt{\frac{x}{\beta y}}} J_0\left(\frac{\bar{\omega}}{M}\sqrt{x^2 - \beta^2y^2\sec^4\theta}\right)d\theta e^{-i\bar{\omega}x}(dx)^2\right] \tag{6}$$

where

$$\bar{\omega} = \frac{M^2\omega}{V\beta^2}$$

Note that the upper limit of the second integral, which is within the brackets of equation (5), will vanish when x equals βy. This indicates that the second integral represents the correction to the "purely supersonic" disturbance potential needed to compensate for the flow around the wing or aileron tip. The first term is the purely supersonic disturbance potential obtained in reference 9.

The indicated integrations in equations (5) and (6) do not appear to be obtainable in terms of known functions. For purposes of evaluation, however, these equations can be expanded in a power series and terms can be retained to any desired power of the frequency parameter $\bar{\omega}$. For region II, the region of "purely supersonic" flow wherein $x \geqq \beta y$, equations (5) and (6), expanded to $\bar{\omega}^5$, yield

$$\phi_\delta = -\frac{V\delta}{\beta} f_1(x_2) \tag{7}$$

$$\phi_{\delta} = -\frac{\dot{\delta}}{\beta} f_2(x_2) \tag{8}$$

where

$$f_1(x) = x - \frac{i\bar{\omega}x^2}{2} - \frac{\bar{\omega}^2x^3}{12M^2}(2\beta^2 + 3) + \frac{i\bar{\omega}^3x^4}{48M^2}(2\beta^2 + 5) + \frac{\bar{\omega}^4x^5}{960M^4}(8\beta^4 + 40\beta^2 + 35) -$$

$$\frac{i\bar{\omega}^5x^6}{5760M^4}(8\beta^4 + 56\beta^2 + 63) \tag{9}$$

$$f_2(x) = \int_0^x f_1(x)dx \tag{10}$$

and $x_2 = x - x_1$. For region I, the region of "mixed supersonic" flow, equations (5) and (6) yield

$$\phi_\delta = -\frac{2bV\delta}{\beta} \lambda_1(x_2,y) \tag{11}$$

$$\phi_{\dot{\delta}} = -\frac{4b^2\dot{\delta}}{\beta} \lambda_2(x_2,y) \tag{12}$$

where

$$\lambda_1(x,y) = \frac{2}{\pi}\left\{F_1 - i\bar{\omega}F_2 - \frac{\bar{\omega}^2}{2M^2}\left(xF_2 + \beta^2F_3\right) + \frac{i\bar{\omega}^3}{12M^2}\left[3x^2F_2 + (2\beta^2 - 1)F_4\right] + \frac{\bar{\omega}^4}{48M^4}\left[x^3(4\beta^2 + 5)F_2 - 3xF_4 + 2\beta^2F_5\right] - \frac{i\bar{\omega}^5}{960M^4}\left[5x^4(4\beta^2 + 7)F_2 - 30x^2F_4 + (8\beta^4 - 4\beta^2 + 3)F_6\right]\right\} \tag{13}$$

$$\lambda_2(x,y) = \int_0^x \lambda_1(x,y)\,dx \tag{14}$$

The functions $f_1(x)$, $f_2(x)$, $\lambda_1(x,y)$, and $\lambda_2(x,y)$ were given to the seventh power of $\bar{\omega}$ in reference 7 and are repeated here to $\bar{\omega}^5$. In equations (13) and (14)

$$F_n(x,y) = \int_0^x x^{n-1} \sin^{-1}\sqrt{\frac{\beta y}{x}}\,dx$$

and

$$\int_0^x x^m F_n(x,y) = \frac{1}{m + 1}\left(x^{m+1} - F_{m+n+1}\right)$$

Further information regarding these F_n functions can be found in references 1 and 4.

The above equations could have been obtained from the equations of references 1 and 4 by substituting δ for α, 0 for x_o, and x_2 for x. In other words, to obtain ϕ_δ and $\phi_{\dot{\delta}}$, the aileron in supersonic flow may be considered as a rectangular wing rotating about its leading edge insofar as regions I and II are concerned.

Region III.- The problem of determining the velocity potential for region III may be complicated by the existence of flow about the inboard tip of the aileron. The present treatment of the problem avoids this complication by assuming the gap between aileron and wing to be sealed as was done in reference 6.

The velocity potential for region III can be obtained from reference 9. In reference 9 the potential of a "mixed supersonic" region at the tip of a rectangular wing in supersonic flow was considered. If this region is assumed to be part of a "purely supersonic" region, an approximation for the velocity potential in region III can be obtained. Although the expression so obtained was an approximation for the velocity potential in the tip region then under consideration, it is precisely the potential for region III of the current problem. This expression, as applied to the present case, is

$$\begin{aligned}\phi = {} & \frac{1}{\beta\pi}\int_0^{x_2} (V\delta + \xi\dot{\delta})e^{-i\bar{\omega}(x_2-\xi)} \int_0^{\pi} \cos\left[\frac{\bar{\omega}}{M}(x_2 - \xi)\sin\theta\right]d\theta\, d\xi - \\ & \frac{1}{\beta\pi}\int_0^{x_2-\beta y_2} (V\delta + \xi\dot{\delta})e^{-i\bar{\omega}(x_2-\xi)} \int_0^{\cos^{-1}\frac{\beta y_2}{x_2-\xi}} \cos\left[\frac{\bar{\omega}}{M}(x_2 - \xi)\sin\theta\right]d\theta\, d\xi \\ = {} & \frac{1}{\beta}\int_0^{x_2} (V\delta + \xi\dot{\delta})e^{-i\bar{\omega}(x_2-\xi)}\, J_0\left[\frac{\bar{\omega}}{M}(x_2 - \xi)\right]d\xi - \\ & \frac{1}{\beta\pi}\int_0^{x_2-\beta y_2} (V\delta + \xi\dot{\delta})e^{-i\bar{\omega}(x_2-\xi)} \int_0^{\cos^{-1}\frac{\beta y_2}{x_2-\xi}} \cos\left[\frac{\bar{\omega}}{M}(x_2 - \xi)\sin\theta\right]d\theta\, d\xi \end{aligned} \tag{15}$$

where

$$y_2 = y_1 - y$$

(This expression for the potential applies to those points of region III that are on the wing as well as those on the control surface.)

The first term on the right-hand side of equation (15) is the sum of the potentials ϕ_δ and $\phi_{\dot{\delta}}$ of the "purely supersonic" region, region II, given in expanded form in equations (7) and (8). The calculation, therefore, of only the second term is necessary. After expansion of equation (15) in a power series to the fifth power of $\bar{\omega}$, the velocity potentials for region III can be expressed as

$$\phi_\delta = -\frac{V\delta}{\beta}\left[\left(\frac{1}{2} + \frac{1}{\pi}\sin^{-1}\frac{\beta y_2}{x_2}\right)f_1(x_2) + \frac{\beta y_2}{\pi}\cosh^{-1}\frac{x_2}{\beta\left|y_2\right|}f_3(y_2) - \frac{\beta y_2}{\pi}\sqrt{x_2^2 - \beta^2 y_2^2}\,\lambda_3(x_2,y_2)\right] \tag{16}$$

$$\phi_{\dot{\delta}} = -\frac{\dot{\delta}}{\beta}\left\{\left(\frac{1}{2} + \frac{1}{\pi}\sin^{-1}\frac{\beta y_2}{x_2}\right)f_2(x_2) + \frac{\beta y_2}{\pi}\cosh^{-1}\frac{x_2}{\beta\left|y_2\right|}\left[x_2 f_3(y_2) + f_4(y_2)\right] - \frac{\beta y_2}{\pi}\sqrt{x_2^2 - \beta^2 y_2^2}\,\lambda_4(x_2,y_2)\right\} \tag{17}$$

where

$$f_3(y_2) = 1 - \frac{\beta^4 y_2^2 \bar{\omega}^2}{12M^2} + \frac{\beta^8 y_2^4 \bar{\omega}^4}{320M^4} \tag{18}$$

$$f_4(y_2) = \frac{i\bar{\omega}\beta^2 y_2^2}{6} - \frac{i\bar{\omega}^3 \beta^6 y_2^4}{80M^2} \tag{19}$$

and

$$\lambda_3(x_2,y_2) = \frac{i\bar{\omega}}{2} + \frac{\bar{\omega}^2 x_2}{12M^2}(\beta^2 + 3) - \frac{i\bar{\omega}^3 x_2^{\ 2}}{144M^2}(2\beta^2 + 17) - \frac{i\bar{\omega}^3\beta^2 y_2^{\ 2}}{72M^2}(2\beta^2 - 1) -$$

$$\frac{\bar{\omega}^4 x_2^{\ 3}}{960M^4}(2\beta^4 + 40\beta^2 + 45) - \frac{\bar{\omega}^4 x_2\beta^2 y_2^{\ 2}}{960M^4}(3\beta^4 - 10) +$$

$$\frac{i\bar{\omega}^5 x_2^{\ 4}}{28800M^4}(8\beta^4 + 296\beta^2 + 453) + \frac{i\bar{\omega}^5 x_2^{\ 2}\beta^2 y_2^{\ 2}}{43200M^4}(16\beta^2 - 8\beta^2 - 219) +$$

$$\frac{i\bar{\omega}^5\beta^4 y_2^{\ 4}}{10800M^4}(8\beta^4 - 4\beta^2 + 3) \qquad (20)$$

$$\lambda_4(x_2,y_2) = \frac{1}{2} + \frac{i\bar{\omega}x_2}{3} + \frac{\bar{\omega}^2 x_2^{\ 2}}{48M^2}(2\beta^2 + 5) - \frac{\bar{\omega}^2\beta^2 y_2^{\ 2}}{24M^2}(2\beta^2 + 1) -$$

$$\frac{i\bar{\omega}^3 x_2^{\ 3}}{720M^2}(4\beta^2 + 25) - \frac{i\bar{\omega}^3 x_2\beta^2 y_2^{\ 2}}{720M^2}(11\beta^2 - 10) -$$

$$\frac{\bar{\omega}^4 x_2^{\ 4}}{5760M^4}(4\beta^4 + 56\beta^2 + 61) - \frac{\bar{\omega}^4 x_2^{\ 2}\beta^2 y_2^{\ 2}}{8640M^4}(11\beta^4 - 8\beta^2 + 43) +$$

$$\frac{\bar{\omega}^4\beta^4 y_2^{\ 4}}{2160M^4}(8\beta^4 + 4\beta^2 - 1) \qquad (21)$$

Other regions.- Two other types of regions are possible. One region is formed when the Mach line from the inboard edge of one aileron intersects the inboard edge of the aileron on the opposite side of the wing. This type is not of practical interest, however, since the interference effects of the fuselage between the ailerons would be of far greater importance. The other type of region, formed when the Mach lines from the tips of one aileron intersect on the aileron, presents no difficulties. The potential in this type region is simply the sum of the expressions for the potential in regions I and III minus the potential for region II. This parallels directly the treatment of region T_3 in reference 1.

Expressions for the velocity potentials due to aileron motion have been provided for all regions in the field of flow of the aileron (see eqs. (7), (8), (11), (12), (16), and (17)). The aforementioned equations are in terms of known integrable functions and, as subsequently shown in the following section, yield force and moment coefficients for a chordwise strip that are valid for sufficiently small values of the parameter $\bar{\omega}$.

Section Forces and Moments

Expressions for section force and moment coefficients for any station along the span are derived. In deriving these expressions the variables x, y, x_o, and x_1 are employed as nondimensional quantities obtained by dividing the variables previously used by the wing chord 2b. The local perturbation pressure difference between the upper and lower surfaces of the wing may be written as

$$\Delta p = -2\rho\left(\frac{\partial\phi}{\partial t} + \frac{V}{2b}\frac{\partial\phi}{\partial x}\right) \tag{22}$$

where ρ is the density of the medium. The section force (positive downward) on the wing is therefore

$$P = 2b\int_0^1 \Delta p \, dx \tag{23}$$

The section moments (positive leading edge up) acting on the wing section about the wing axis of rotation x_o and on the aileron section about the hinge point x_1 are, respectively,

$$M_\alpha = 4b^2 \int_0^1 (x - x_o)\Delta p \, dx \tag{24}$$

$$M_\delta = 4b^2 \int_{x_1}^1 (x - x_1)\Delta p \, dx \tag{25}$$

After substituting equations (3) and (22) into equations (23), (24), and (25) and performing the indicated integrations, the results may be written as

$$\left.\begin{aligned}
P &= -4\rho bV^2k^2\left[\frac{h}{b}(L_1 + iL_2) + \alpha(L_3 + iL_4) + \delta(L_5 + iL_6)\right] = -\rho V^2 bc_l \\
M_\alpha &= -4\rho b^2V^2k^2\left[\frac{h}{b}(M_1 + iM_2) + \alpha(M_3 + iM_4) + \delta(M_5 + iM_6)\right] = 2\rho V^2b^2c_m \\
M_\delta &= -4\rho b^2V^2k^2\left[\frac{h}{b}(N_1 + iN_2) + \alpha(N_3 + iN_4) + \delta(N_5 + iN_6)\right] \\
&= 2(1 - x_1)^2\rho V^2b^2c_h
\end{aligned}\right\} \tag{26}$$

The terms L_i, M_i, and N_i (where $i = 1, 2, \ldots 6$) are the in-phase and out-of-phase components of the force and moment coefficients; the odd-number subscripts are the in-phase components and the even-number subscripts are the out-of-phase components. Terms with subscripts 1 and 2 are associated only with vertical translations of the wing. Terms with subscripts 3 and 4 are associated with angular position and rotation of the wing about $x = x_o$. Indices 5 and 6 are associated with the angular position and rotation of the control surface about $x = x_1$. As may be seen from equation (26), the forms L_i, M_i, and N_i, which have been used in studies of unsteady flow, can be readily converted to the conventional section coefficients for lift c_l, pitching moment c_m, and aileron hinge moment c_h.

Expressions for the coefficients of equation (26) differ for the various regions of the wing and aileron. Coefficients associated with wing motion, namely L_1, L_2, L_3, L_4, M_1, M_2, M_3, and M_4, were given to the third power of the frequency parameter $\bar{\omega}$ in reference 1 and were extended to the seventh power in reference 4. For completeness, however, these expressions are repeated to the fifth power of $\bar{\omega}$ in the appendix to this paper.

The remaining coefficients can be divided into two groups: (1) those which show the effect of wing motions h and α upon the aileron moment M_δ, namely N_1, N_2, N_3, and N_4, and (2) the aileron section coefficients due to the aileron potentials ϕ_δ and $\phi_{\dot{\delta}}$, namely L_5, L_6, M_5, M_6, N_5, and N_6. Expressions for the coefficients in each of these groups for the various regions of the wing-aileron combination will now be given.

Aileron coefficients N_1, N_2, N_3, N_4 due to wing motion.- For the section coefficients N_1, N_2, N_3, and N_4, the aileron is divided into three regions (fig. 2). Region 1 includes all sections outboard of the point where the wing-tip Mach line crosses the aileron hinge, region 3 comprises all sections inboard of the point where this Mach line crosses the trailing edge, and region 2 includes all intermediate sections. The coefficients can be expressed as follows:

$$\left.\begin{aligned}
N_1 &= N_1' + M_1' - 2x_1L_1' \\
N_2 &= N_2' + M_2' - 2x_1L_2' \\
N_3 &= N_3' - 2x_oN_1 \\
N_4 &= N_4' - 2x_oN_2
\end{aligned}\right\} \tag{27}$$

where the coefficients M_i' and L_i' $(i = 1, 2, 3, 4)$ refer to the wing coefficients given in the appendix for $x_o = 0$.

For region 1 where $0 < y < x_1/\beta$, the coefficients of equation (27) are calculated by using the expressions for the wing coefficients presented in the appendix (eqs. (A1) and (A2)) for the region $0 < y < 1/\beta$ and are given as the following expressions:

$$
\left.
\begin{aligned}
N_1' &= -\frac{4}{\beta\pi}\left\{x_1^2F_1'' - \frac{2x_1}{\beta^2}(2\beta^2 + 1)F_2'' + \frac{3\beta^2 + 2}{\beta^2}F_3'' + \right. \\
&\quad \left. \frac{2M^2k^2}{3\beta^6}\left[x_1^3F_2'' - 3x_1^2\beta^4F_3'' + (8\beta^4 + 4\beta^2 - 1)x_1F_4'' - \beta^2(5\beta^2 + 4)F_5''\right]\right\} \\
N_2' &= \frac{4}{\beta\pi}\left\{\frac{1}{k}(x_1F_1'' - F_2'') + \frac{M^2k}{\beta^4}\left[(2\beta^2 - 1)x_1^2F_2'' - 6\beta^2x_1F_3'' + (4\beta^2 + 1)F_4''\right] + \right. \\
&\quad \left. \frac{M^4k^3}{\beta^8}\left[5x_1^4F_2'' - 2x_1^2(8\beta^4 - 4\beta^2 + 3)F_4'' + 40\beta^4x_1F_5'' - (24\beta^4 + 8\beta^2 - 1)F_6''\right]\right\} \\
N_3' &= M_3' - 2x_1L_3' + \frac{4}{\beta\pi}\left\{\frac{1}{k^2}(x_1F_1'' - F_2'') - \frac{2x_1^3}{3}F_1'' + \right. \\
&\quad \frac{x_1^2}{\beta^4}F_2''(6\beta^4 + 3\beta^2 - 1) - \frac{2F_3''}{\beta^2}x_1(6\beta^2 + 5) + \frac{F_4''}{3\beta^4}(20\beta^4 + 21\beta^2 + 3) + \\
&\quad \frac{M^2k^2}{12\beta^8}\left[x_1^4F_2''(\beta^2 + 5) + 16\beta^6x_1^3F_3'' - 2x_1^2F_4''(40\beta^6 + 20\beta^4 - 5\beta^2 + 3) + \right. \\
&\quad \left.\left. 8\beta^4x_1F_5''(15\beta^2 + 13) - (56\beta^6 + 64\beta^4 + 11\beta^2 - 1)F_6''\right]\right\} \\
N_4' &= M_4' - 2x_1L_4' + \frac{4}{\beta\pi}\left\{\frac{2}{\beta^2k}\left[\beta^2x_1^2F_1'' - x_1F_2''(3\beta^2 + 1) + (2\beta^2 + 1)F_3''\right] + \right. \\
&\quad \frac{2kM^2}{3\beta^6}\left[x_1^3F_2''(2\beta^4 - \beta^2 + 1) - 12x_1^2\beta^4F_3'' + x_1F_4''(20\beta^4 + 7\beta^2 - 1) - \right. \\
&\quad \left. 2\beta^2F_5''(5\beta^2 + 3)\right] - \frac{M^4k^3}{90\beta^{10}}\left[3x_1^5F_2''(\beta^2 + 7) + 10x_1^3F_4''(8\beta^6 - 4\beta^4 + \right. \\
&\quad 3\beta^2 - 3) - 360\beta^6x_1^2F_5'' + 3x_1F_6''(168\beta^6 + 64\beta^4 - 11\beta^2 + 3) - \\
&\quad \left.\left. 8\beta^4F_7''(28\beta^2 + 19)\right]\right\}
\end{aligned}
\right\} \quad (28)
$$

where

$$F_n'' = \int_0^{x_1} x^{n-1} \sin^{-1}\sqrt{\frac{\beta y}{x}}\, dx$$

For region 2 where $x_1/\beta < y < 1/\beta$, the terms in equation (27) are calculated by again using the expressions for the wing coefficients presented in the appendix (eqs. (A1) and (A2)) for the region $0 < y < 1/\beta$ and yield the following expressions:

$$\left.\begin{aligned}
N_1' &= \frac{2x_1^3}{3\beta^3} - \frac{4\beta^2 + 5}{15\beta^7} M^2k^2x_1^5 \\
N_2' &= \frac{x_1^2}{\beta k} - \frac{M^2kx_1^4}{2\beta^5} + \frac{M^4k^3x_1^6}{36\beta^9}(4\beta^2 + 7) \\
N_3' &= M_3' - 2x_1L_3' + \frac{x_1^2}{\beta k^2} - \frac{x_1^4}{6\beta^5}(\beta^2 + 3) + \frac{M^2k^2x_1^6}{180\beta^9}(4\beta^4 + 35\beta^2 + 35) \\
N_4' &= M_4' - 2x_1L_4' + \frac{2x_1^3}{3\beta^3k}(\beta^2 - 1) + \frac{M^2kx_1^5}{15\beta^7}(\beta^2 + 5) - \\
&\quad \frac{M^4k^3x_1^7}{630\beta^{11}}(4\beta^4 + 49\beta^2 + 63)
\end{aligned}\right\} \quad (29)$$

For region 3 where $1/\beta < y$, the terms of equation (27) are obtained by using the wing coefficients in the appendix (eqs. (A3) and (A4)) for the region $y > 1/\beta$ and equation (29).

<u>Aileron coefficients L_5, L_6, M_5, M_6, N_5, N_6 due to aileron motion</u>.- The expressions for the aileron coefficients L_5, L_6, M_5, M_6, N_5, and N_6 depend upon which region (see fig. 1) contains the trailing edge of the section.

For a section partly in region I, that is $0 < y < x_3/\beta$ (where $x_3 = 1 - x_1$), the coefficients are

$$
\left.
\begin{aligned}
L_5 &= \frac{4}{\beta\pi}\left\{\frac{F_1'''}{2k^2} - x_3{}^2F_1''' + \frac{x_3F_2'''}{\beta^4}(6\beta^4 + 3\beta^2 - 1) - \frac{F_3'''}{\beta^2}(6\beta^2 + 5) + \frac{k^2M^2}{6\beta^8}\Big[x_3{}^3F_2'''(\beta^2 + 5) + 12\beta^6x_3{}^2F_3''' - \right.\\
&\qquad \left. x_3F_4'''(40\beta^6 + 20\beta^4 - 5\beta^2 + 3) + 2\beta^4F_5'''(15\beta^2 + 13)\Big]\right\}\\
L_6 &= \frac{4}{\beta\pi}\left\{\frac{1}{k}\left[2x_3F_1''' - \frac{F_2'''}{\beta^2}(3\beta^2 + 1)\right] + \frac{kM^2}{3\beta^6}\Big[3x_3{}^2F_2'''(2\beta^4 - \beta^2 + 1) - 24\beta^4x_3F_3''' + F_4'''(20\beta^4 + 7\beta^2 - 1)\Big] - \right.\\
&\qquad \left. \frac{k^3M^4}{60\beta^{10}}\Big[5x_3{}^4F_2'''(\beta^2 + 7) + 10x_3{}^2F_4'''(8\beta^6 - 4\beta^4 + 3\beta^2 - 3) - 240\beta^6x_3F_5''' + F_6'''(168\beta^6 + 64\beta^4 - 11\beta^2 + 3)\Big]\right\}\\
M_5 &= \frac{4}{\beta\pi}\left\{\frac{F_2'''}{k^2} - \frac{4x_3{}^3F_1'''}{3} + \frac{x_3{}^2F_2'''}{\beta^4}(6\beta^4 + 3\beta^2 - 1) - \frac{F_4'''}{3\beta^4}(20\beta^4 + 21\beta^2 + 3) + \frac{k^2M^2}{12\beta^8}\Big[3(\beta^2 + 5)x_3{}^4F_2''' + \right.\\
&\qquad \left. 32\beta^6x_3{}^3F_3''' - 2x_3{}^2F_4'''(40\beta^6 + 20\beta^4 - 5\beta^2 + 3) + F_6'''(56\beta^6 + 64\beta^4 + 11\beta^2 - 1)\Big]\right\} + 2(x_1 - x_o)L_5\\
M_6 &= \frac{4}{\beta\pi}\left\{\frac{2}{k\beta^2}\left[\beta^2x_3{}^2F_1''' - (2\beta^2 + 1)F_3'''\right] + \frac{2kM^2}{3\beta^6}\Big[2x_3{}^3F_2'''(2\beta^4 - \beta^2 + 1) - 12\beta^4x_3{}^2F_3''' + 2\beta^2F_5'''(5\beta^2 + 3)\Big] - \right.\\
&\qquad \left. \frac{2k^3M^4}{45\beta^{10}}\Big[3x_3{}^5F_2'''(\beta^2 + 7) + 5x_3{}^3F_4'''(8\beta^6 - 4\beta^4 + 3\beta^2 - 3) - 90\beta^6x_3{}^2F_5''' + 2\beta^4F_7'''(28\beta^2 + 19)\Big]\right\} + 2(x_1 - x_o)L_6\\
N_5 &= M_5 - 2(x_1 - x_o)L_5\\
N_6 &= M_6 - 2(x_1 - x_o)L_6
\end{aligned}
\right\} \quad (30)
$$

where

$$F_n''' = \int_0^{x_3} x^{n-1} \sin^{-1}\sqrt{\frac{\beta y}{x}}\,dx$$

For a section entirely within region II, that is $\frac{x_3}{\beta} < y < y_1 - \frac{x_3}{\beta}$, these coefficients become

$$\left.\begin{aligned}
L_5 &= \frac{x_3}{\beta k^2} - \frac{x_3^3}{3\beta^5}(\beta^2 + 3) + \frac{k^2M^2x_3^5}{60\beta^9}(4\beta^4 + 35\beta^2 + 35) \\
L_6 &= \frac{x_3^2}{k\beta^3}(\beta^2 - 1) + \frac{kM^2x_3^4}{6\beta^7}(\beta^2 + 5) - \frac{k^3M^4x_3^6}{180\beta^{11}}(4\beta^4 + 49\beta^2 + 63) \\
M_5 &= \frac{x_3^2}{\beta k^2} - \frac{x_3^4}{2\beta^5}(\beta^2 + 3) + \frac{k^2M^2x_3^6}{36\beta^9}(4\beta^4 + 35\beta^2 + 35) + 2(x_1 - x_o)L_5 \\
M_6 &= \frac{4x_3^3}{3k\beta^3}(\beta^2 - 1) + \frac{4M^2kx_3^5}{15\beta^7}(\beta^2 + 5) - \frac{M^4k^3x_3^7}{105\beta^{11}}(4\beta^4 + 49\beta^2 + 63) + \\
&\quad 2(x_1 - x_o)L_6 \\
N_5 &= M_5 - 2(x_1 - x_o)L_5 \\
N_6 &= M_6 - 2(x_1 - x_o)L_6
\end{aligned}\right\} \quad (31)$$

For a section partly within region III, that is $y_1 - \frac{x_3}{\beta} < y < y_1 + \frac{x_3}{\beta}$, these coefficients become

$$L_5 = \left[\frac{x_3}{\beta k^2} - \frac{x_3^3}{3\beta^5}(\beta^2 + 3) + \frac{k^2M^2x_3^5}{60\beta^9}(4\beta^4 + 35\beta^2 + 35)\right]\left(\frac{1}{2} + \frac{1}{\pi}\sin^{-1}\frac{\beta y_2}{x_3}\right) + \frac{y_2}{\pi}\cosh^{-1}\frac{x_3}{\beta y_2}\left[\frac{1}{k^2} - 2x_3^2 - \frac{y_2^2}{3}(6\beta^2 + 5) + \frac{2M^2k^2y_2^2x_3^2}{3} + \frac{M^2k^2y_2^4}{20}(15\beta^2 + 13)\right] + \frac{x_3y_2}{\pi}\sqrt{x_3^2 - \beta^2y_2^2}\left[\frac{1}{3\beta^4}(12\beta^4 + 4\beta^2 - 3) + \frac{M^2k^2x_3^2}{180\beta^8}(10\beta^6 - 22\beta^4 + 55\beta^2 + 135) - \frac{M^2k^2y_2^2}{180\beta^6}(265\beta^6 + 83\beta^4 - 50\beta^2 + 30)\right] \tag{32a}$$

$$L_6 = \left[\frac{x_3^2}{k\beta^3}(\beta^2 - 1) + \frac{kM^2x_3^4}{6\beta^7}(\beta^2 + 5) - \frac{k^3M^4x_3^6}{180\beta^{11}}(4\beta^4 + 49\beta^2 + 63)\right]\left(\frac{1}{2} + \frac{1}{\pi}\sin^{-1}\frac{\beta y_2}{x_3}\right) + \frac{x_3y_2}{\pi}\cosh^{-1}\frac{x_3}{\beta y_2}\left[\frac{4}{k} - \frac{8M^2ky_2^2}{3} + \frac{3M^4k^3y_2^4}{5}\right] - \frac{y_2}{\pi}\sqrt{x_3^2 - \beta^2y_2^2}\left[\frac{3\beta^2 + 1}{\beta^2k} - \frac{kM^2x_3^2}{18\beta^6}(18\beta^4 - 11\beta^2 + 17) - \frac{kM^2y_2^2}{9\beta^4}(20\beta^4 + 7\beta^2 - 1) + \frac{M^4k^3x_3^4}{900\beta^{10}}(8\beta^6 - 36\beta^4 + 139\beta^2 + 453) + \frac{M^4k^3x_3^2y_2^2}{180\beta^8}(126\beta^6 - 172\beta^4 + 203\beta^2 - 219) + \frac{2M^4k^3y_2^4}{675\beta^6}(168\beta^6 + 64\beta^4 - 11\beta^2 + 3)\right] \tag{32b}$$

$$M_5 = \left[\frac{x_3^2}{\beta k^2} - \frac{x_3^4}{2\beta^5}(\beta^2 + 3) + \frac{k^2M^2x_3^6}{36\beta^9}(4\beta^4 + 35\beta^2 + 35)\right]\left(\frac{1}{2} + \frac{1}{\pi}\sin^{-1}\frac{\beta y_2}{x_3}\right) -$$

$$\frac{8y_2x_3^3}{3\pi}\cosh^{-1}\frac{x_3}{\beta y_2}\left(1 - \frac{M^2k^2y_2^2}{3}\right) + \frac{y_2}{\pi}\sqrt{x_3^2 - \beta^2y_2^2}\left[\frac{1}{k^2} + \frac{x_3^2}{18\beta^4}(88\beta^4 + \right.$$

$$33\beta^2 - 21) - \frac{y_2^2}{9\beta^2}(20\beta^4 + 21\beta^2 + 3) + \frac{M^2k^2x_3^4}{180\beta^8}(16\beta^6 - 36\beta^4 + 81\beta^2 + 209) -$$

$$\frac{M^2k^2x_3^2y_2^2}{270\beta^6}(488\beta^6 + 172\beta^4 - 97\beta^2 + 47) + \frac{2M^2k^2y_2^4}{135\beta^4}(56\beta^6 + 64\beta^4 +$$

$$\left.11\beta^2 - 1)\right] + 2(x_1 - x_o)L_5 \qquad (32c)$$

$$M_6 = \left[\frac{4x_3^3}{3k\beta^3}(\beta^2 - 1) + \frac{4M^2kx_3^5}{15\beta^7}(\beta^2 + 5) - \frac{M^4k^3x_3^7}{105\beta^{11}}(4\beta^4 + 49\beta^2 + 63)\right]\left(\frac{1}{2} + \right.$$

$$\left.\frac{1}{\pi}\sin^{-1}\frac{\beta y_2}{x_3}\right) + \frac{y_2}{\pi}\cosh^{-1}\frac{x_3}{\beta y_2}\left[\frac{4x_3^2}{k} - \frac{2y_2^2}{3k}(2\beta^2 + 1) - \frac{8M^2kx_3^2y_2^2}{3} + \right.$$

$$\left.\frac{3M^4k^3x_3^2y_2^4}{5} - \frac{M^4k^3y_2^6}{126}(28\beta^2 + 19)\right] - \frac{x_3y_2}{\pi}\sqrt{x_3^2 - \beta^2y_2^2}\left[\frac{2}{3\beta^2k}(2\beta^2 + 1) - \right.$$

$$\frac{2M^2kx_3^2}{15\beta^6}(5\beta^4 - 7\beta^2 + 10) - \frac{M^2ky_2^2}{5\beta^2}(5\beta^2 + 3) + \frac{M^4k^3x_3^4}{945\beta^{10}}(14\beta^6 - 64\beta^4 +$$

$$231\beta^2 + 777) + \frac{M^4k^3x_3^2y_2^2}{945\beta^8}(133\beta^6 - 185\beta^4 + 210\beta^2 - 210) +$$

$$\left.\frac{M^4k^3y_2^4}{126\beta^2}(28\beta^2 + 19)\right] + 2(x_1 - x_o)L_6 \qquad (32d)$$

$$N_5 = M_5 - 2(x_1 - x_o)L_5 \tag{32e}$$

$$N_6 = M_6 - 2(x_1 - x_o)L_6 \tag{32f}$$

Equations (32) apply to all sections of region III - those sections on the wing as well as those on the aileron.

The case of a section in a region within the Mach cones from both aileron-leading-edge tips $y_1 - \frac{x_3}{\beta} < y < \frac{x_3}{\beta}$, which is formed when the Mach lines intersect on the aileron, can be treated with the expressions provided in this section. The coefficients for such a section are obtained by adding the corresponding expressions of equations (30) and (32) and subtracting the pertinent expression of equations (31).

Total Forces and Moments

In order to gain some insight into overall effects of aileron location and aspect ratio, expressions for total forces and moments are provided. The total lift, total wing moment, and total aileron moment, respectively, can be written as

$$\left.\begin{aligned}
\bar{P} &= -8\rho b^2V^2k^2A\left[\frac{h}{b}(\bar{L}_1 + i\bar{L}_2) + \alpha(\bar{L}_3 + i\bar{L}_4) + \frac{y_1}{bA}\delta(\bar{L}_5 + i\bar{L}_6)\right] \\
\bar{M}_\alpha &= -8\rho b^3V^2k^2A\left[\frac{h}{b}(\bar{M}_1 + i\bar{M}_2) + \alpha(\bar{M}_3 + i\bar{M}_4) + \frac{y_1}{bA}\delta(\bar{M}_5 + i\bar{M}_6)\right] \\
\bar{M}_\delta &= -8\rho b^3V^2k^2\frac{y_1}{b}\left[\frac{h}{b}(\bar{N}_1 + i\bar{N}_2) + \alpha(\bar{N}_3 + i\bar{N}_4) + \delta(\bar{N}_5 + i\bar{N}_6)\right]
\end{aligned}\right\} \tag{33}$$

where A is the wing aspect ratio. Expressions for the coefficients $\bar{L}_1$, $\bar{L}_2$, $\bar{L}_3$, $\bar{L}_4$, $\bar{M}_1$, $\bar{M}_2$, $\bar{M}_3$, and $\bar{M}_4$ in equations (33) are given to the seventh power of the frequency in reference 4. For completeness they are provided to the fifth power of the frequency in the appendix.

The other coefficients associated with wing motion are

$$\bar{N}_1 = \left[\frac{2x_1{}^3}{3\beta^3} - \frac{M^2k^2x_1{}^5}{15\beta^7}(4\beta^2 + 5)\right] - \frac{b}{3y_1}\left[\frac{x_1{}^4}{2\beta^4}(\beta^2 + 2) - \frac{M^2k^2x_1{}^6}{15\beta^8}(\beta^4 + 8\beta^2 + 8)\right] + \bar{M}_1{}' - 2(x_1 - x_o)\bar{L}_1{}' \tag{34a}$$

$$\bar{N}_2 = \left[\frac{x_1{}^2}{\beta k} - \frac{M^2kx_1{}^4}{2\beta^5} + \frac{M^4k^3x_1{}^6}{36\beta^9}(4\beta^2 + 7)\right] - \frac{b}{3y_1}\left[\frac{x_1{}^3}{\beta^2k} - \frac{M^2kx_1{}^5}{5\beta^6}(\beta^2 + 4) + \frac{2M^4k^3x_1{}^7}{105\beta^{10}}(\beta^4 + 12\beta^2 + 16)\right] + \bar{M}_2{}' - 2(x_1 - x_o)\bar{L}_2{}' \tag{34b}$$

$$\bar{N}_3 = \left[\frac{x_1{}^2}{\beta k^2} - \frac{x_1{}^4}{6\beta^5}(\beta^2 + 3) + \frac{M^2k^2x_1{}^6}{180\beta^9}(4\beta^4 + 35\beta^2 + 35)\right] - \frac{b}{3y_1}\left[\frac{x_1{}^3}{\beta^2k^2} - \frac{x_1{}^5}{5\beta^6}(3\beta^2 + 4) + \frac{2M^2k^2x_1{}^7}{105\beta^{10}}(5\beta^4 + 20\beta^2 + 16)\right] + \bar{M}_3{}' - 2(x_1 - x_o)(\bar{L}_3{}' + 2x_o\bar{L}_1{}') - 2x_o(\bar{N}_1 - \bar{M}_1{}') \tag{34c}$$

$$\bar{N}_4 = \left[\frac{2x_1{}^3}{3\beta^3k}(\beta^2 - 1) + \frac{M^2kx_1{}^5}{15\beta^7}(\beta^2 + 5) - \frac{M^4k^3x_1{}^7}{630\beta^{11}}(4\beta^4 + 49\beta^2 + 63)\right] + \frac{b}{3y_1}\left[\frac{x_1{}^4}{\beta^4k} - \frac{4kM^2x_1{}^6}{15\beta^8}(\beta^2 + 2) + \frac{M^4k^3x_1{}^8}{105\beta^{12}}(3\beta^4 + 16\beta^2 + 16)\right] + \bar{M}_4{}' - 2(x_1 - x_o)(\bar{L}_4{}' + 2x_o\bar{L}_2{}') - 2x_o(\bar{N}_2 - \bar{M}_2{}') \tag{34d}$$

The primed coefficients employed in equations (34) are obtained by replacing the wing aspect ratio A with y_1/b in the corresponding unprimed coefficients in equations (A5) and (A6) of the appendix. The remaining coefficients, which are associated with the total forces and moments on the aileron, are

$$\left.\begin{aligned}
\bar{L}_5 &= \left[\frac{x_3}{\beta k^2} - \frac{x_3^3}{3\beta^5}(\beta^2 + 3) + \frac{k^2M^2x_3^5}{60\beta^9}(4\beta^4 + 35\beta^2 + 35)\right] - \frac{b}{2y_1}\left(1 + \frac{2}{\pi}\right)\left[\frac{x_3^2}{\beta^2k^2} - \right. \\
&\quad \left. \frac{x_3^4}{3\beta^6}(3\beta^2 + 4) + \frac{2M^2k^2x_3^6}{45\beta^{10}}(5\beta^4 + 20\beta^2 + 16)\right] \\
\bar{L}_6 &= \left[\frac{x_3^2}{\beta^3k}(\beta^2 - 1) + \frac{kM^2x_3^4}{6\beta^7}(\beta^2 + 5) - \frac{k^3M^4x_3^6}{180\beta^{11}}(4\beta^4 + 49\beta^2 + 63)\right] + \\
&\quad \frac{b}{3y_1}\left(1 + \frac{2}{\pi}\right)\left[\frac{2x_3^3}{\beta^4k} - \frac{4M^2kx_3^5}{5\beta^8}(\beta^2 + 2) + \frac{4M^4k^3x_3^7}{105\beta^{12}}(3\beta^4 + 16\beta^2 + 16)\right] \\
\bar{M}_5 &= \left[\frac{x_3^2}{\beta k^2} - \frac{x_3^4}{2\beta^5}(\beta^2 + 3) + \frac{k^2M^2x_3^6}{36\beta^9}(4\beta^4 + 35\beta^2 + 35)\right] - \frac{b}{3y_1}\left(1 + \frac{2}{\pi}\right)\left[\frac{2x_3^3}{\beta^2k^2} - \right. \\
&\quad \left. \frac{4x_3^5}{5\beta^6}(3\beta^2 + 4) + \frac{4k^2M^2x_3^7}{35\beta^{10}}(5\beta^4 + 20\beta^2 + 16)\right] + 2(x_1 - x_o)\bar{L}_5 \\
\bar{M}_6 &= \left[\frac{4x_3^3}{3k\beta^3}(\beta^2 - 1) + \frac{4M^2kx_3^5}{15\beta^7}(\beta^2 + 5) - \frac{M^4k^3x_3^7}{105\beta^{11}}(4\beta^4 + 49\beta^2 + 63)\right] + \\
&\quad \frac{b}{3y_1}\left(1 + \frac{2}{\pi}\right)\left[\frac{3x_3^4}{k\beta^4} - \frac{4kM^2x_3^6}{3\beta^8}(\beta^2 + 2) + \frac{M^4k^3x_3^8}{15\beta^{12}}(3\beta^4 + 16\beta^2 + 16)\right] + \\
&\quad 2(x_1 - x_o)\bar{L}_6 \\
\bar{N}_5 &= \bar{M}_5 - 2(x_1 - x_o)\bar{L}_5 \\
\bar{N}_6 &= \bar{M}_6 - 2(x_1 - x_o)\bar{L}_6
\end{aligned}\right\} \quad (35)$$

In equations (35) the expression within the first set of brackets in each equation represents the component of the coefficient due to two-dimensional flow, and the second term provides the corrections for edge effects. The correction for the inboard or sealed edge is $2/\pi$ times that for the outboard edge of the aileron. This serves as a check on the calculations, inasmuch as it is in accord with the observations of references 6 and 9. Equations (35) do not include the contribution of the part of region III that is off the aileron. If this contribution were included, thereby providing overall total coefficients for the wing-aileron combination, the correction for the inboard edge would vanish. For an aileron whose outboard as well as inboard edge can be considered sealed, the expression $1 + \frac{2}{\pi}$ in equations (35) should be replaced by $4/\pi$.

CALCULATIONS AND DISCUSSION

Spanwise Aerodynamic Effects

To give some indication as to the general nature of the spanwise distribution of the different components of the lift and moment coefficients introduced by the presence of a control surface, these components were evaluated for a given set of conditions at different spanwise locations. This spanwise variation is illustrated in figure 3 for an aileron, with a chord one-half of the wing chord and a span one-fourth of the wing span, mounted adjacent to the wing tip on a wing of aspect ratio 4 at a Mach number of 1.3 and a reduced frequency k of 1/9. Figure 3(a) presents the spanwise distribution of the components which contribute to the wing lift force and moment, and figure 3(b) presents the distribution of the components contributing to the aileron hinge moment. Two-dimensional values of the coefficients are represented by dashed lines. For the aforementioned set of conditions, the Mach lines from the aileron tips intersect on the aileron. (For stations partly within the region formed by these intersecting Mach lines, see the discussion following eqs. (32)).

Application to Flutter

The application of the section force and moment coefficients developed in this paper to some particular examples of the flutter of a finite-span wing with partial-span control surfaces is considered of interest. A broad systematic study, however, such as that of reference 10 which employed two-dimensional aerodynamic theory, is beyond the scope of the present paper.

The particular examples deal with a rectangular wing-aileron of aspect ratio 4 at a Mach number of 1.3. This wing, without an aileron, has been analyzed for flutter and the flutter characteristics have been calculated and compared with experiment at $M = 1.3$ in reference 11, where two-dimensional flow coefficients were employed, and in reference 12, where finite-span coefficients were employed (refer to model A-1 results of the reference papers). The following pertinent parameters of reference 11 are used:

Aspect ratio, A 4.0
Elastic-axis location, x_o, referred to 2b 0.413
Center-of-gravity location of wing-aileron combination, x_α, measured from elastic axis in semichords 0.156
Radius of gyration of wing-aileron combination, $r_\alpha = \sqrt{I_\alpha/mb^2}$, referred to x_o 0.28
First natural frequency in bending, ω_h, radians/sec 838
First natural frequency in torsion, ω_α, radians/sec 1,747
Density parameter, $1/\kappa = m/\pi\rho b^2$ 64.9

The present study considers the wing described above to have an aileron, hinged about its leading edge, with a chord one-half the wing chord and a span one-fourth the wing span. The aileron is considered rigid but spring restrained at the hinge. The effect upon flutter of varying the spanwise location of this aileron is examined for two mass-balance conditions. The aileron parameters assumed for this study are

y_1/b 2
Aileron-hinge location, x_1, referred to 2b 0.5
Reduced aileron center-of-gravity location, x_β, measured from hinge in wing semichords . . . . 0.2 and 0
Reduced radius of gyration of aileron, $r_\beta = \sqrt{I_\beta/mb^2}$, referred to x_1 . . . . 0.125 and 0.1

Flutter analyses for three degrees of freedom in three-dimensional flow.- Three degrees of freedom - namely, wing bending, wing torsion, and aileron rotation - are involved in the present study. By the method given in chapter IX of reference 13, the flutter determinantal equation for the three degrees of freedom involved may be written as

$$\begin{vmatrix} A_{hh} & A_{h\alpha} & A_{h\beta} \\ A_{\alpha h} & A_{\alpha\alpha} & A_{\alpha\beta} \\ A_{\beta h} & A_{\beta\alpha} & A_{\beta\beta} \end{vmatrix} = 0 \tag{36}$$

where the determinant elements are

$$\left.\begin{aligned}
A_{hh} &= \left[1 - \left(\frac{\omega_h}{\omega}\right)^2\right] \int_0^1 Z_h^2 dy - \frac{4}{\pi} \kappa \int_0^1 (L_1' + iL_2) Z_h^2 dy \\
A_{h\alpha} &= x_\alpha \int_0^1 Z_h Z_\alpha \, dy - \frac{4}{\pi} \kappa \int_0^1 (L_3 + iL_4) Z_h Z_\alpha \, dy \\
A_{h\beta} &= x_\beta \int_{l_1}^{l_2} Z_h Z_\beta \, dy - \frac{4}{\pi} \kappa \int_{l_1}^{l_2} (L_5 + iL_6) Z_h Z_\beta \, dy \\
A_{\alpha h} &= x_\alpha \int_0^1 Z_\alpha Z_h \, dy - \frac{4}{\pi} \kappa \int_0^1 (M_1 + iM_2) Z_\alpha Z_h \, dy \\
A_{\alpha\alpha} &= r_\alpha^2 \left[1 - \left(\frac{\omega_\alpha}{\omega}\right)^2\right] \int_0^1 Z_\alpha^2 dy - \frac{4}{\pi} \kappa \int_0^1 (M_3 + iM_4) Z_\alpha^2 dy \\
A_{\alpha\beta} &= \left[r_\beta^2 + 2x_\beta(x_1 - x_o)\right] \int_{l_1}^{l_2} Z_\alpha Z_\beta \, dy - \frac{4}{\pi} \kappa \int_{l_1}^{l_2} (M_5 + iM_6) Z_\alpha Z_\beta \, dy \\
A_{\beta h} &= x_\beta \int_{l_1}^{l_2} Z_\beta Z_h \, dy - \frac{4}{\pi} \kappa \int_{l_1}^{l_2} (N_1 + iN_2) Z_\beta Z_h \, dy \\
A_{\beta\alpha} &= \left[r_\beta^2 + 2x_\beta(x_1 - x_o)\right] \int_{l_1}^{l_2} Z_\beta Z_\alpha \, dy - \frac{4}{\pi} \kappa \int_{l_1}^{l_2} (N_3 + iN_4) Z_\beta Z_\alpha \, dy \\
A_{\beta\beta} &= r_\beta^2 \left[1 - \left(\frac{\omega_\delta}{\omega}\right)^2\right] \int_{l_1}^{l_2} Z_\beta^2 dy - \frac{4}{\pi} \kappa \int_{l_1}^{l_2} (N_5 + iN_6) Z_\beta^2 \, dy
\end{aligned}\right\} \tag{37}$$

and where l_1 and l_2 represent, respectively, the inboard and outboard edges of the aileron, Z_h, Z_α, Z_β represent, respectively, the mode shapes in wing bending, wing torsion, and aileron rotation, and the coefficients L_i, M_i, N_i are defined in equation (26). In this analysis the wing modes Z_h and Z_α were assumed to be the uncoupled first bending and first torsion modes of a uniform cantilever beam, while the aileron mode was assumed to be unity. The aerodynamic integrals required in these equations are obtained by numerical integration employing the basic method shown in appendix B of reference 4.

After substitution of these integrals and parameters into the determinant elements, the equations are solved, as in chapter XIII of reference 13, at several values of the reduced frequency k for the flutter frequency ω and aileron frequency ω_δ. The results are presented as plots of the parameter $b\omega_h/c$ against the natural frequency ratio ω_δ/ω_h in figures 4 and 5. The parameter $b\omega_h/c$ is employed here as in reference 10, since it is preferable in a compressibility study rather than the velocity parameter normally used in incompressible flow. The choice of ω_h rather than ω_α in this parameter is purely arbitrary since in this analysis ω_h/ω_α is constant.

Figure 4 illustrates the results of the flutter analysis for the mass-balance condition defined by the parameters $x_\beta = 0.2$ and $r_\beta{}^2 = 0.125$ implying a relatively rearward aileron center-of-gravity location. The analysis was performed with the aileron in three spanwise locations on the wing, as shown in figure 4. In figure 4(a) the aileron is in the inboard position adjacent to the wing center line. In figure 4(b) the aileron is located midway between the wing center line and the wing tip and in figure 4(c), adjacent to the wing tip.

Two curves appear on these plots and regions of instability relative to each curve are shown. The lower curve extends through the entire range of the frequency ratio ω_δ/ω_h and is associated with a mode that is predominantly a combination of wing bending and wing torsion. As ω_δ becomes infinite, the case of coupled wing bending torsion is approached; the value of $b\omega_h/c$ approached asymptotically is indicated by the short-dashed line and corresponds to the result from reference 12. As ω_δ decreases the value of $b\omega_h/c$ increases slightly. At a sufficiently low value of ω_δ a point is reached where the region of instability associated with the upper curve appears. Since the stiffness $b\omega_h/c$ associated with this upper curve is higher than that associated with the lower curve, the mode associated with the upper curve is the critical one for low values of the frequency parameter ω_δ/ω_h.

In figure 4 parts of the curves are estimated as indicated by the long-dashed lines. Over the estimated portion of the curve the reduced-frequency parameter k is greater than 0.25 and beyond this value the aerodynamic derivatives developed in the present paper become inadequate.

To provide some indication of the effects of mass balance, the configurations of figures 4(b) and 4(c) are again analyzed for the mass-balance condition defined by the parameters $x_\beta = 0$ and $r_\beta{}^2 = 0.100$, which places the aileron center of gravity at the hinge. These results are shown in figure 5 where only the cases of the aileron at the midspan location (fig. 5(a)) and at the outboard location (fig. 5(b)) are considered.

For figure 5(a) the maximum value of ω_δ/ω_h for the upper curve is unknown and hence this curve is not closed. A comparison of figures 5(b) (balanced aileron) and 4(c) (unbalanced aileron) shows that the upper curve is extended to a much higher value of ω_δ/ω_h in figure 5(b), and indicates that a stiffer (higher frequency) aileron is required for stability. This finding is in accordance with an observation of reference 10 that mass balance may have an adverse effect for low supersonic Mach numbers.

Two-degree-of-freedom subcases.- It is often deemed practical in examining the problem of flutter for a multidegree-of-freedom configuration to consider pertinent subcases under the assumption that the characteristics of the solution to the multidegree-of-freedom problem will manifest themselves in the solutions to the pertinent subcases at some saving in labor. To test this assumption the subcases of the present three-degree-of-freedom problem which involve aileron motion - that is, the wing-bending—aileron-rotation case and the wing-torsion—aileron-rotation case - have been considered.

The flutter determinants are obtained for the bending-aileron case by eliminating the row and column associated with wing torsion from the three-degree-of-freedom flutter determinants employed in the previous sections. Similarly for the torsion-aileron case, the row and column associated with wing bending are eliminated. The results of this study are shown in figures 6 and 7.

The results obtained by using the finite-span coefficients of the present paper for both mass-balance conditions are presented for the wing-bending—aileron subcase in figure 6 and for the wing-torsion—aileron subcase in figure 7. The curves in figure 6 have the same form as the upper curves in figures 4 and 5 and, about the same critical ranges of $b\omega_h/c$. For the aileron at an outboard location a comparison of figure 6(c) with figures 4(c) and 5(b) provides a somewhat interesting observation; namely, that, when only two degrees of freedom are considered, the critical frequency ratio for the first mass-balance condition is increased, whereas for the second or mass-balanced condition the critical frequency seems to be slightly decreased.

In figure 7 are presented the results for the torsion-aileron case. No region of instability was detected for the aileron in the inboard case. Therefore, results are presented only for the midspan location (fig. 7(a)) and outboard location (fig. 7(b)). The curves in these figures appear to correspond in form to the lower curves in figures 4 and 5. Whereas mass balancing the aileron did not appear to materially affect this stability boundary when three degrees of freedom were considered, for the mode under consideration a mass-balance control surface would seem detrimental from a flutter standpoint when only two degrees of freedom are considered.

CONCLUDING REMARKS

The present paper has extended the treatment of NACA Rep. 1028 and NACA TN 3076 for rectangular wings in supersonic flow to include a third degree of freedom, namely partial-span aileron rotation. Expressions for the velocity potential and consequent section forces and moments for the aileron have been provided to the fifth power of a frequency parameter. In addition total force and moment coefficients have been obtained.

The section coefficients were applied to a particular flutter study which attempted to compare:

(a) The flutter characteristics for the aileron in various spanwise locations

(b) The flutter characteristics of mass-balanced and mass-unbalanced ailerons

(c) The flutter properties as determined from a three-degree-of-freedom problem with properties obtained from the two-degree-of-freedom subcases

Because of the rather limited nature of this study (for example, no Mach number investigation was made, only two mass-balance conditions were employed, and only one density ratio was employed), the results of this investigation were not intended to be construed as conclusive but should aid in suggesting topics for future investigation.

With regard to the spanwise location of the aileron upon the flutter characteristics of the wing, no conclusion can readily be drawn other than that the inboard location of the aileron is best from a flutter standpoint. The possible detrimental effect of applying mass balance to the control surface in this Mach number region, shown in NACA TN 3160, was also indicated in this study, especially where three degrees of freedom were considered. Where finite-span considerations were applied to the two-degree-of-freedom subcases, mass balance appeared to be beneficial from a flutter standpoint for the wing-bending—aileron case but not for the wing-torsion—aileron case. The results of the two-degree-of-freedom subcases appeared to reflect the flutter properties obtained from the three-degree-of-freedom problem.

Langley Aeronautical Laboratory,
National Advisory Committee for Aeronautics,
Langley Field, Va., February 9, 1956.

APPENDIX A

COEFFICIENTS ASSOCIATED WITH WING MOTION

Most of the expressions in this appendix have been taken from reference 4, where they were presented as a power series containing terms up to the seventh power of the frequency parameter $\bar{\omega}$. Inasmuch as the present paper considers expansions to the fifth power of the frequency parameter, the expressions of reference 4 are accordingly abridged. These abridged expressions are repeated here for the sake of completeness.

Section Coefficients Associated With Wing Motion

For sections between the wing tip and the point where the leading-edge Mach line intersects the trailing edge, $0 < y < 1/\beta$, the section coefficients are:

$$
\left.
\begin{aligned}
L_1 &= -\frac{4}{\beta\pi}\left\{\bar{\bar{F}}_1 - \bar{\bar{F}}_2\frac{(2\beta^2+1)}{\beta^2} + \frac{M^2k^2}{3\beta^6}\left[3\bar{\bar{F}}_2 - 6\beta^4\bar{\bar{F}}_3 + (8\beta^4+4\beta^2-1)\bar{\bar{F}}_4\right]\right\} = L_1' \\
L_2 &= \frac{4}{\beta\pi}\left\{\frac{\bar{\bar{F}}_1}{2k} + \frac{M^2k}{\beta^4}\left[(2\beta^2-1)\bar{\bar{F}}_2 - 3\beta^2\bar{\bar{F}}_3\right] + \frac{M^4k^3}{6\beta^8}\left[5\bar{\bar{F}}_2 - (8\beta^4-4\beta^2+3)\bar{\bar{F}}_4 + 10\beta^4\bar{\bar{F}}_5\right]\right\} = L_2' \\
L_3 &= \frac{4}{\beta\pi}\left\{\frac{\bar{\bar{F}}_1}{2k^2} - \bar{\bar{F}}_1 + \frac{1}{\beta^4}\left[(6\beta^4+3\beta^2-1)\bar{\bar{F}}_2 - \beta^2(6\beta^2+5)\bar{\bar{F}}_3\right] + \frac{M^2k^2}{6\beta^8}\left[(\beta^2+5)\bar{\bar{F}}_2 + 12\beta^6\bar{\bar{F}}_3 - \right.\right. \\
&\qquad \left.\left.(40\beta^6+20\beta^4-5\beta^2+3)\bar{\bar{F}}_4 + 2\beta^4(15\beta^2+13)\bar{\bar{F}}_5\right]\right\} - 2x_oL_1 \\
&= L_3' - 2x_oL_1' \\
L_4 &= \frac{4}{\beta\pi}\left\{\frac{1}{\beta^2k}\left[2\beta^2\bar{\bar{F}}_1 - (3\beta^2+1)\bar{\bar{F}}_2\right] + \frac{M^2k}{3\beta^6}\left[3(2\beta^4-\beta^2+1)\bar{\bar{F}}_2 - 24\beta^4\bar{\bar{F}}_3 + (20\beta^4+7\beta^2-1)\bar{\bar{F}}_4\right] - \right. \\
&\qquad \left.\frac{M^4k^3}{60\beta^{10}}\left[5(\beta^2+7)\bar{\bar{F}}_2 + 10(8\beta^6-4\beta^4+3\beta^2-3)\bar{\bar{F}}_4 - 240\beta^6\bar{\bar{F}}_5 + (168\beta^6+64\beta^4-11\beta^2+3)\bar{\bar{F}}_6\right]\right\} - 2x_oL_2 \\
&= L_4' - 2x_oL_2'
\end{aligned}
\right\} \quad (A1)
$$

$$
\left.
\begin{aligned}
M_1 &= -\frac{4}{\beta\pi}\left\{\bar{\bar{F}}_1 - \frac{\bar{\bar{F}}_3}{\beta^2}(3\beta^2 + 2) + \frac{2M^2k^2}{3\beta^6}\left[2\bar{\bar{F}}_2 - 3\beta^4\bar{\bar{F}}_3 + \beta^2(5\beta^2 + 4)\bar{\bar{F}}_5\right]\right\} - 2x_oL_1 \\
&= M_1' - 2x_oL_1' \\
M_2 &= \frac{4}{\beta\pi}\left\{\frac{1}{k}\bar{\bar{F}}_2 + \frac{M^2k}{\beta^4}\left[(2\beta^2 - 1)\bar{\bar{F}}_2 - (4\beta^2 + 1)\bar{\bar{F}}_4\right] + \frac{M^4k^3}{12\beta^8}\left[15\bar{\bar{F}}_2 - 2(8\beta^4 - 4\beta^2 + 3)\bar{\bar{F}}_4 + (24\beta^4 + 8\beta^2 - 1)\bar{\bar{F}}_6\right]\right\} - 2x_oL_2 \\
&= M_2' - 2x_oL_2' \\
M_3 &= \frac{4}{\beta\pi}\left\{\frac{1}{k^2}\bar{\bar{F}}_2 - \frac{4}{3}\bar{\bar{F}}_1 + \frac{1}{\beta^4}(6\beta^4 + 3\beta^2 - 1)\bar{\bar{F}}_2 - \frac{1}{3\beta^4}(20\beta^4 + 21\beta^2 + 3)\bar{\bar{F}}_4 + \frac{M^2k^2}{12\beta^8}\left[3(\beta^2 + 5)\bar{\bar{F}}_2 + 32\beta^6\bar{\bar{F}}_3 - \right.\right. \\
&\qquad \left.\left. 2(40\beta^6 + 20\beta^4 - 5\beta^2 + 3)\bar{\bar{F}}_4 + (56\beta^6 + 64\beta^4 + 11\beta^2 - 1)\bar{\bar{F}}_6\right]\right\} - 2x_o\left(M_1 + L_3 + 2x_oL_1\right) \\
&= M_3' - 2x_o(M_1' + L_3' - 2x_oL_1') \\
M_4 &= \frac{4}{\beta\pi}\left\{\frac{2}{\beta^2k}\left[\beta^2\bar{\bar{F}}_1 - (2\beta^2 + 1)\bar{\bar{F}}_3\right] + \frac{4kM^2}{3\beta^6}\left[(2\beta^4 - \beta^2 + 1)\bar{\bar{F}}_2 - 6\beta^4\bar{\bar{F}}_3 + \beta^2(5\beta^2 + 3)\bar{\bar{F}}_5\right] - \frac{2M^4k^3}{45\beta^{10}}\left[3(\beta^2 + 7)\bar{\bar{F}}_2 + \right.\right. \\
&\qquad \left.\left. 5(8\beta^6 - 4\beta^4 + 3\beta^2 - 3)\bar{\bar{F}}_4 - 90\beta^6\bar{\bar{F}}_5 + 2\beta^4(28\beta^2 + 19)\bar{\bar{F}}_7\right]\right\} - 2x_o(M_2 + L_4 + 2x_oL_2) \\
&= M_4' - 2x_o(M_2' + L_4' - 2x_oL_2')
\end{aligned}
\right\} \quad (A2)
$$

In equations (A2)

$$
\bar{\bar{F}}_n = F_n(1,y)
$$

For sections inboard of the point where the leading-edge Mach line intersects the trailing edge, $1/\beta < y$, the section coefficients are:

$$
\left.
\begin{aligned}
L_1 &= \frac{1}{\beta^3} - \frac{M^2k^2}{6\beta^7}(4\beta^2 + 5) = L_1' \\
L_2 &= \frac{1}{\beta k} - \frac{M^2k}{\beta^5} + \frac{M^4k^3}{12\beta^9}(4\beta^2 + 7) = L_2' \\
L_3 &= \frac{1}{\beta k^2} - \frac{1}{3\beta^5}(\beta^2 + 3) + \frac{M^2k^2}{60\beta^9}(4\beta^4 + 35\beta^2 + 35) - 2x_oL_1 = L_3' - 2x_oL_1' \\
L_4 &= \frac{1}{\beta^3k}(\beta^2 - 1) + \frac{M^2k}{6\beta^7}(\beta^2 + 5) - \frac{M^4k^3}{180\beta^{11}}(4\beta^4 + 49\beta^2 + 63) - 2x_oL_2 = L_4' - 2x_oL_2'
\end{aligned}
\right\} (A3)
$$

$$\left.\begin{aligned}
M_1 &= \frac{4}{3\beta^3} - \frac{4M^2k^2}{15\beta^7}(4\beta^2 + 5) - 2x_oL_1 \\
&= M_1' - 2x_oL_1' \\
M_2 &= \frac{1}{\beta k} - \frac{3M^2k}{2\beta^5} + \frac{5M^4k^3}{36\beta^9}(4\beta^2 + 7) - 2x_oL_2 \\
&= M_2' - 2x_oL_2' \\
M_3 &= \frac{1}{\beta k^2} - \frac{1}{2\beta^5}(\beta^2 + 3) + \frac{M^2k^2}{36\beta^9}(4\beta^4 + 35\beta^2 + 35) - 2x_o(M_1 + L_3 + 2x_oL_1) \\
&= M_3' - 2x_o(M_1' + L_3' - 2x_oL_1') \\
M_4 &= \frac{4}{3\beta^3k}(\beta^2 - 1) + \frac{4M^2k}{15\beta^7}(\beta^2 + 5) - \frac{M^4k^3}{105\beta^{11}}(4\beta^4 + 49\beta^2 + 63) - \\
&\quad 2x_o(M_2 + L_4 + 2x_oL_2) \\
&= M_4' - 2x_o(M_2' + L_4' - 2x_oL_2')
\end{aligned}\right\} \quad (A4)$$

Total Coefficients Associated With Wing Motion

Expressions for the coefficients of equations (33) not provided in the body of the paper are as follows:

$$\left.\begin{aligned}
\bar{L}_1 &= \left[\frac{1}{\beta^3} - \frac{M^2k^2}{6\beta^7}(4\beta^2 + 5)\right] - \frac{1}{3A}\left[\frac{\beta^2 + 2}{\beta^4} - \frac{M^2k^2}{5\beta^8}(\beta^4 + 8\beta^2 + 8)\right] \\
\bar{L}_2 &= \left[\frac{1}{\beta k} - \frac{M^2k}{\beta^5} + \frac{M^4k^3}{12\beta^9}(4\beta^2 + 7)\right] - \frac{1}{2A}\left[\frac{1}{\beta^2k} - \frac{M^2k}{3\beta^6}(\beta^2 + 4) + \right. \\
&\qquad \left.\frac{2M^4k^3}{45\beta^{10}}(\beta^4 + 12\beta^2 + 16)\right] \\
\bar{L}_3 &= \left[\frac{1}{\beta k^2} - \frac{1}{3\beta^5}(\beta^2 + 3) + \frac{M^2k^2}{60\beta^9}(4\beta^4 + 35\beta^2 + 35)\right] - \frac{1}{2A}\left[\frac{1}{\beta^2k^2} - \right. \\
&\qquad \left.\frac{1}{3\beta^6}(\beta^2 + 4) + \frac{2M^2k^2}{45\beta^{10}}(5\beta^4 + 20\beta^2 + 16)\right] - 2x_o\bar{L}_1 \\
\bar{L}_4 &= \left[\frac{1}{\beta^3k}(\beta^2 - 1) + \frac{M^2k}{6\beta^7}(\beta^2 + 5) - \frac{M^4k^3}{180\beta^{11}}(4\beta^4 + 49\beta^2 + 63)\right] + \frac{1}{3A}\left[\frac{2}{\beta^4k} - \right. \\
&\qquad \left.\frac{4M^2k}{5\beta^8}(\beta^2 + 2) + \frac{4M^4k^3}{105\beta^{12}}(3\beta^4 + 16\beta^2 + 16)\right] - 2x_o\bar{L}_2
\end{aligned}\right\} \quad (A5)$$

$$\left.\begin{aligned}
\bar{M}_1 &= \left[\frac{4}{3\beta^3} - \frac{4M^2k^2}{15\beta^7}(4\beta^2 + 5)\right] - \frac{1}{3A}\left[\frac{3}{2\beta^4}(\beta^2 + 2) - \frac{M^2k^2}{3\beta^8}(\beta^4 + 8\beta^2 + 8)\right] - 2x_o\bar{L}_1 \\
\bar{M}_2 &= \left[\frac{1}{\beta k} - \frac{3M^2k}{2\beta^5} + \frac{5M^4k^3}{36\beta^9}(4\beta^2 + 7)\right] - \frac{1}{3A}\left[\frac{2}{\beta^2k} - \frac{4M^2k}{5\beta^6}(\beta^2 + 4) + \right. \\
&\qquad \left.\frac{4M^4k^3}{35\beta^{10}}(\beta^4 + 12\beta^2 + 16)\right] - 2x_o\bar{L}_2 \\
\bar{M}_3 &= \left[\frac{1}{\beta k^2} - \frac{1}{2\beta^5}(\beta^2 + 3) + \frac{M^2k^2}{36\beta^9}(4\beta^4 + 35\beta^2 + 35)\right] - \frac{1}{3A}\left[\frac{2}{\beta^2k^2} - \right. \\
&\qquad \left.\frac{4}{5\beta^6}(3\beta^2 + 4) + \frac{4M^2k^2}{35\beta^{10}}(5\beta^4 + 20\beta^2 + 16)\right] - 2x_o(\bar{M}_1 + \bar{L}_3 + 2x_o\bar{L}_1) \\
\bar{M}_4 &= \left[\frac{4}{3\beta^3k}(\beta^2 - 1) + \frac{4M^2k}{15\beta^7}(\beta^2 + 5) - \frac{M^4k^3}{105\beta^{11}}(4\beta^4 + 49\beta^2 + 63)\right] + \frac{1}{3A}\left[\frac{3}{\beta^4k} - \right. \\
&\qquad \left.\frac{4M^2k}{3\beta^8}(\beta^2 + 2) + \frac{M^4k^3}{15\beta^{12}}(3\beta^4 + 16\beta^2 + 16)\right] - 2x_o(\bar{M}_2 + \bar{L}_4 + 2x_o\bar{L}_2)
\end{aligned}\right\} \quad (A6)$$

REFERENCES

1. Watkins, Charles E.: Effect of Aspect Ratio on the Air Forces and Moments of Harmonically Oscillating Thin Rectangular Wings in Supersonic Potential Flow. NACA Rep. 1028, 1951.

2. Miles, John W.: The Oscillating Rectangular Airfoil at Supersonic Speeds. TM RRB-15, U. S. Naval Ordnance Test Station (Inyokern, Calif.), June 1, 1949.

3. Stewartson, K.: On Linearized Potential Theory of Unsteady Supersonic Motion. Quart. Jour. Mech. and Appl. Math., vol. III, pt. 2, 1950, pp. 182-199.

4. Nelson, Herbert C., Rainey, Ruby A., and Watkins, Charles E.: Lift and Moment Coefficients Expanded to the Seventh Power of Frequency for Oscillating Rectangular Wings in Supersonic Flow and Applied to a Specific Flutter Problem. NACA TN 3076, 1954.

5. Tucker, Warren A., and Nelson, Robert L.: Theoretical Characteristics in Supersonic Flow of Constant-Chord Partial-Span Control Surfaces on Rectangular Wings Having Finite Thickness. NACA TN 1708, 1948.

6. Miles, John W.: The Oscillating Rectangular Control Surface at Supersonic Speeds. NAVORD Rep. 1185 (NOTS 241), U. S. Naval Ord. Test Station (Inyokern, Calif.), Oct. 4, 1949.

7. Miles, John W., Naiman, Irven, and Schroedter, G. M.: Aerodynamic Derivatives for an Oscillating Rectangular Airfoil at Supersonic Speeds. NAVORD Rep. 1292 (NOTS 362), U. S. Naval Ord. Test Station, Inyokern, (China Lake, Calif.), Mar. 6, 1951.

8. Churchill, Ruel V.: Modern Operational Mathematics in Engineering. McGraw-Hill Book Co., Inc., 1944.

9. Garrick, I. E., and Rubinow, S. I.: Theoretical Study of Air Forces on an Oscillating or Steady Thin Wing in a Supersonic Main Stream. NACA Rep. 872, 1947. (Supersedes NACA TN 1383.)

10. Woolston, Donald S., and Huckel, Vera: A Calculation Study of Wing-Aileron Flutter in Two Degrees of Freedom for Two-Dimensional Supersonic Flow. NACA TN 3160, 1954.

11. Tuovila, W. J., Baker, John E., and Regier, Arthur A.: Initial Experiments on Flutter of Unswept Cantilever Wings at Mach Number 1.3. NACA TN 3312, 1954. (Supersedes NACA RM L8J11.)

12. Nelson, Herbert C., and Rainey, Ruby A.: Comparison of Flutter Calculations Using Various Aerodynamic Coefficients With Experimental Results for Some Rectangular Cantilever Wings at Mach Number 1.3. NACA TN 3301, 1954.

13. Scanlan, Robert H., and Rosenbaum, Robert: Introduction to the Study of Aircraft Vibration and Flutter. The Macmillan Co., 1951, pp. 205-226, 265-297.

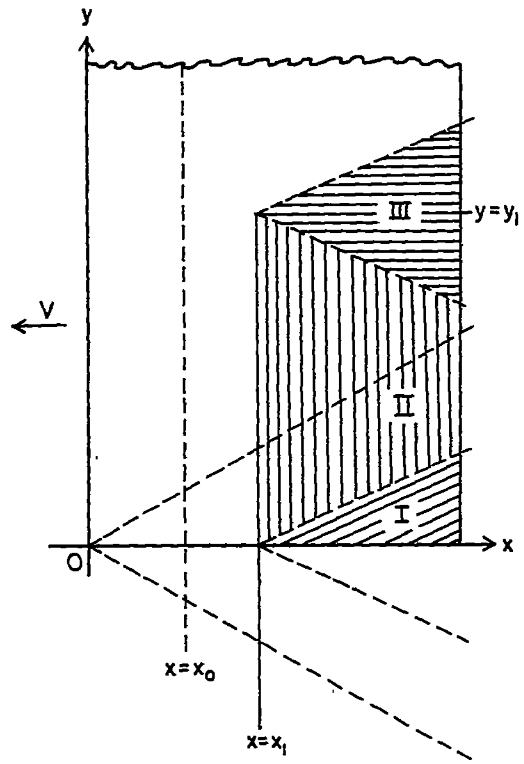

(a) Plan form (xy-plane).

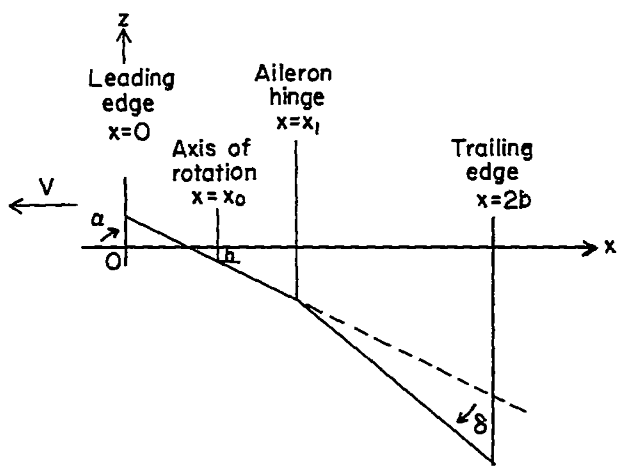

(b) Section through aileron (xz-plane).

Figure 1.- Sketch illustrating coordinate system and degrees of freedom of rectangular wing-aileron configuration.

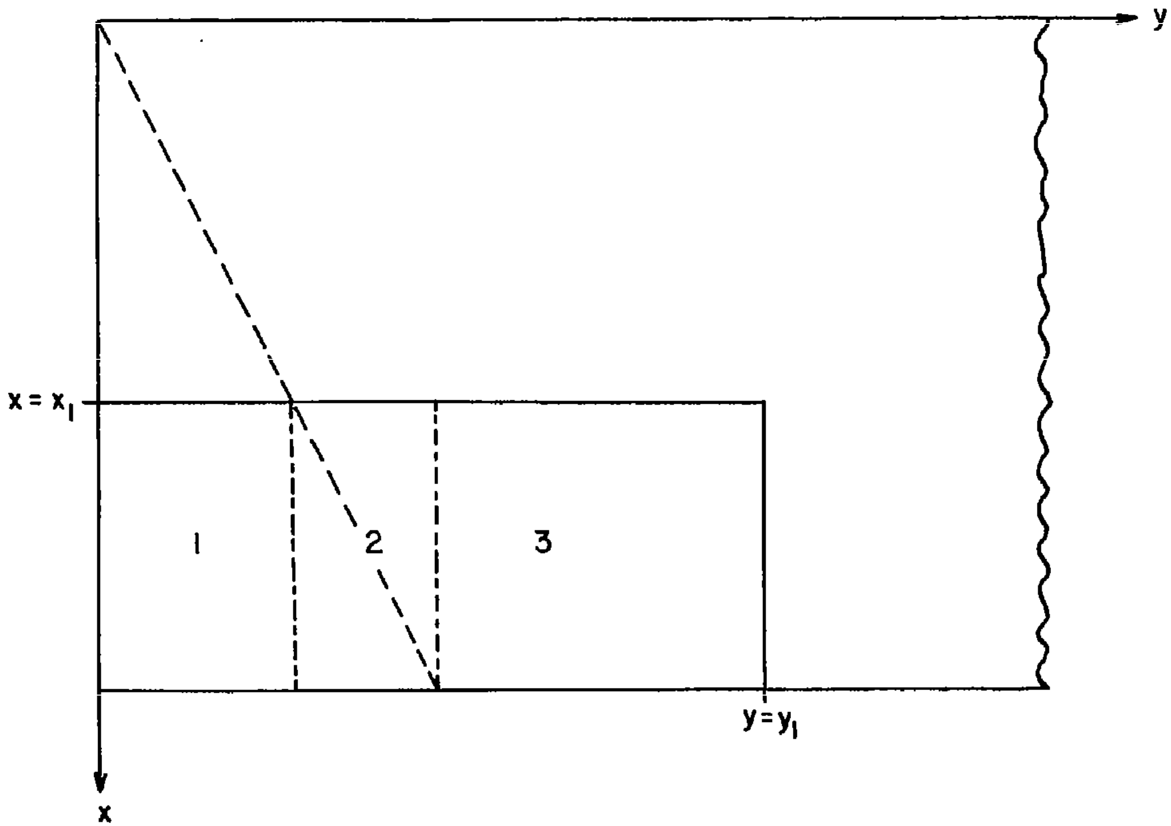

Figure 2.- The regions of the aileron pertinent to the calculation of section coefficients N_1, N_2, N_3, and N_4.

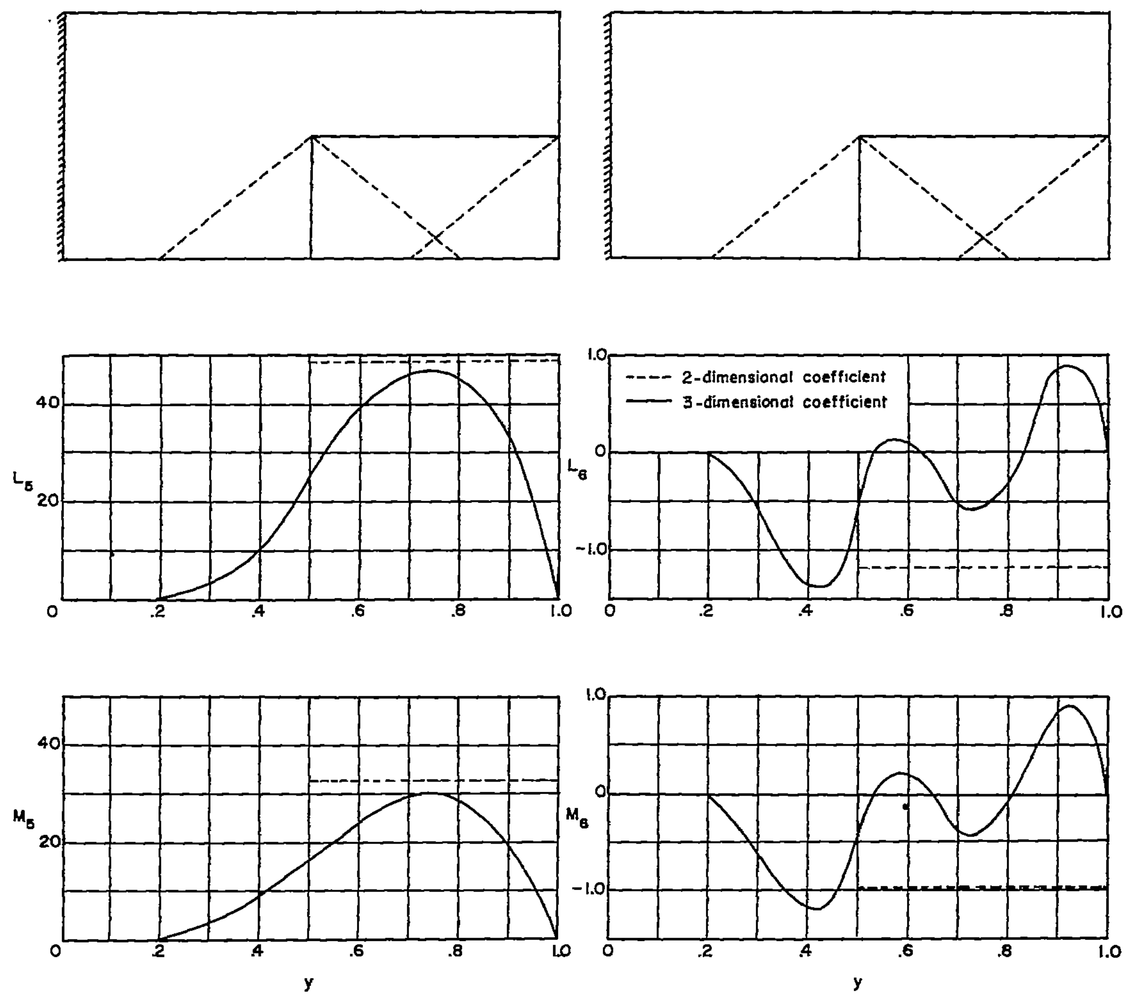

(a) Coefficients contributing to wing lift force and moment.

Figure 3.- Spanwise distribution of components of lift-force and moment coefficients introduced by the presence of a control surface. $M = 1.3$; $k = 1/9$; $A = 4$; and $y_1/b = 2$.

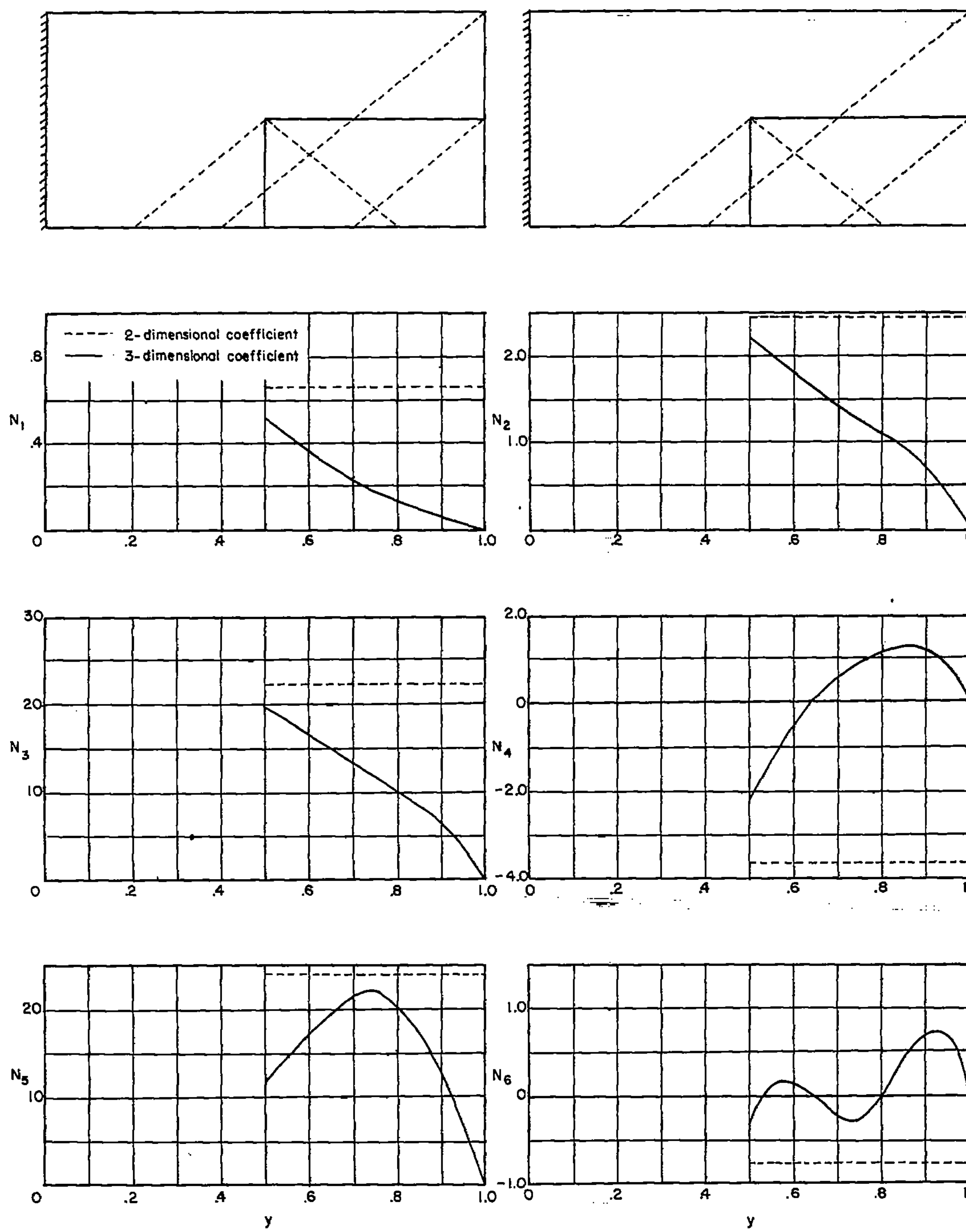

(b) Coefficients contributing to aileron hinge moment.

Figure 3.- Concluded.

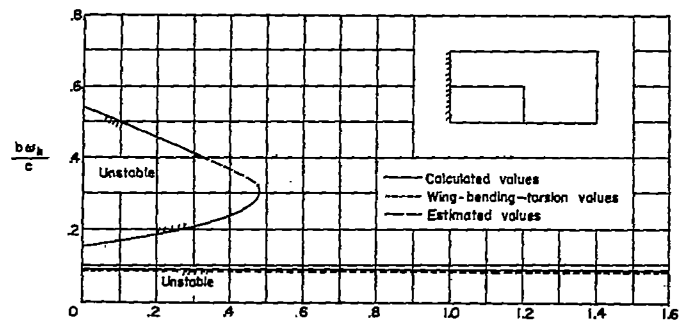

(a) Aileron at inboard location.

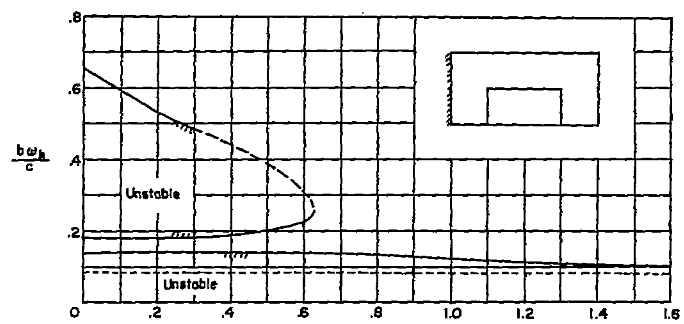

(b) Aileron at midspan location.

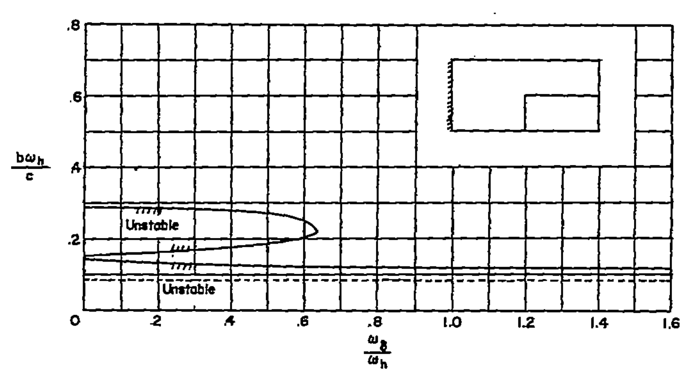

(c) Aileron at outboard location.

Figure 4.- Flutter parameter $b\omega_h/c$ plotted against frequency ratio ω_δ/ω_h for various aileron locations. Three degrees of freedom; $M = 1.3$; $x_\beta = 0.2$; $r_\beta{}^2 = 0.125$. (Other parameters for wing and aileron are given in the text.)

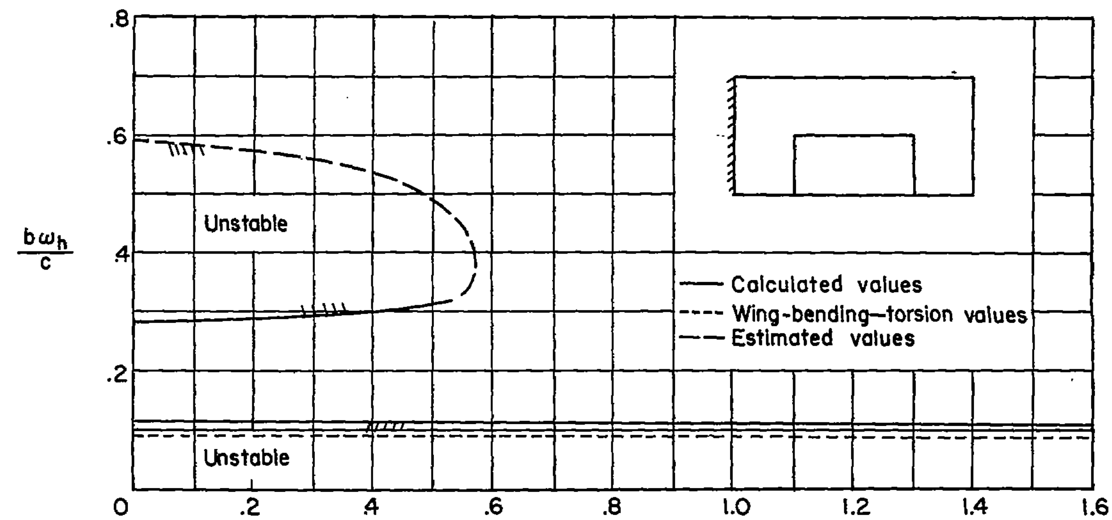

(a) Aileron at midspan location.

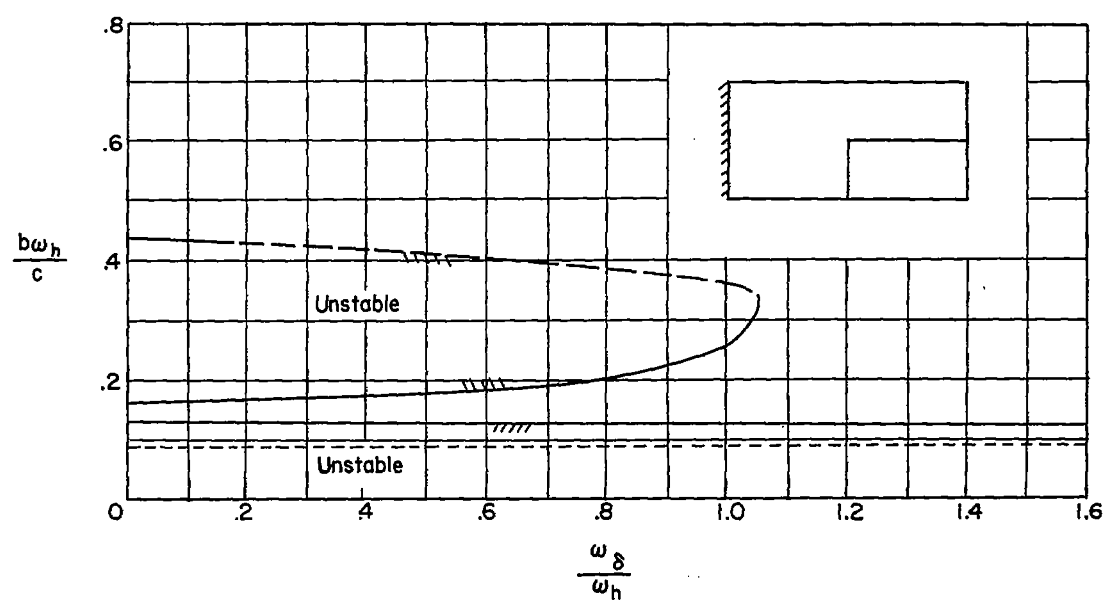

(b) Aileron at outboard location.

Figure 5.- Flutter parameter $b\omega_h/c$ plotted against frequency ratio ω_δ/ω_h for various aileron locations. Three degrees of freedom; $M = 1.3$; $x_\beta = 0$; $r_\beta{}^2 = 0.100$. (Other parameters for wing and aileron are given in the text.)

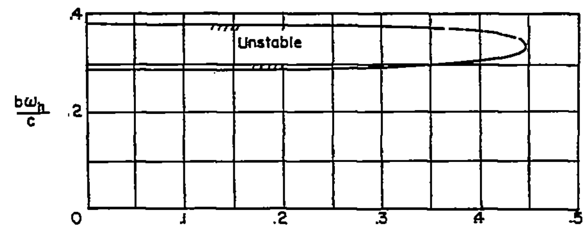

(a) Aileron at inboard location.

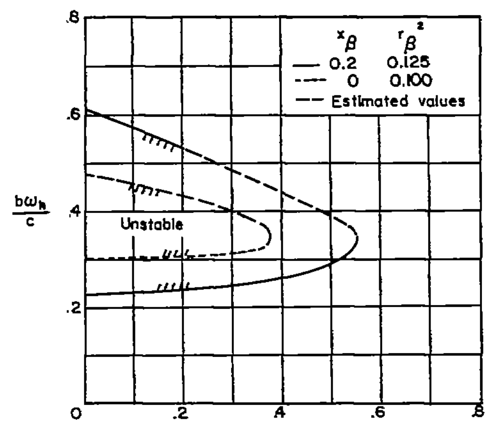

(b) Aileron at midspan location.

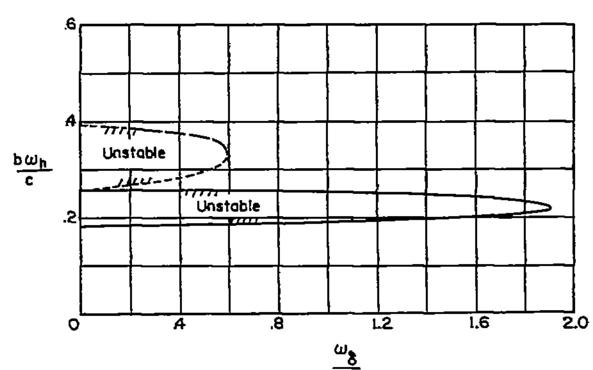

(c) Aileron at outboard location.

Figure 6.- Flutter parameter $b\omega_h/c$ plotted against frequency ratio ω_δ/ω_h for wing-bending—aileron case employing finite-span theory. $M = 1.3$.

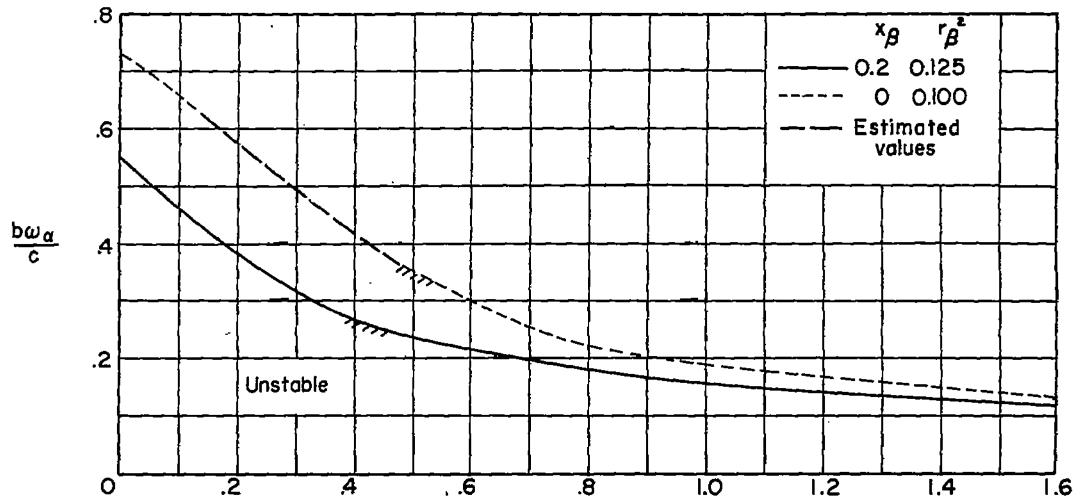

(a) Aileron at midspan location.

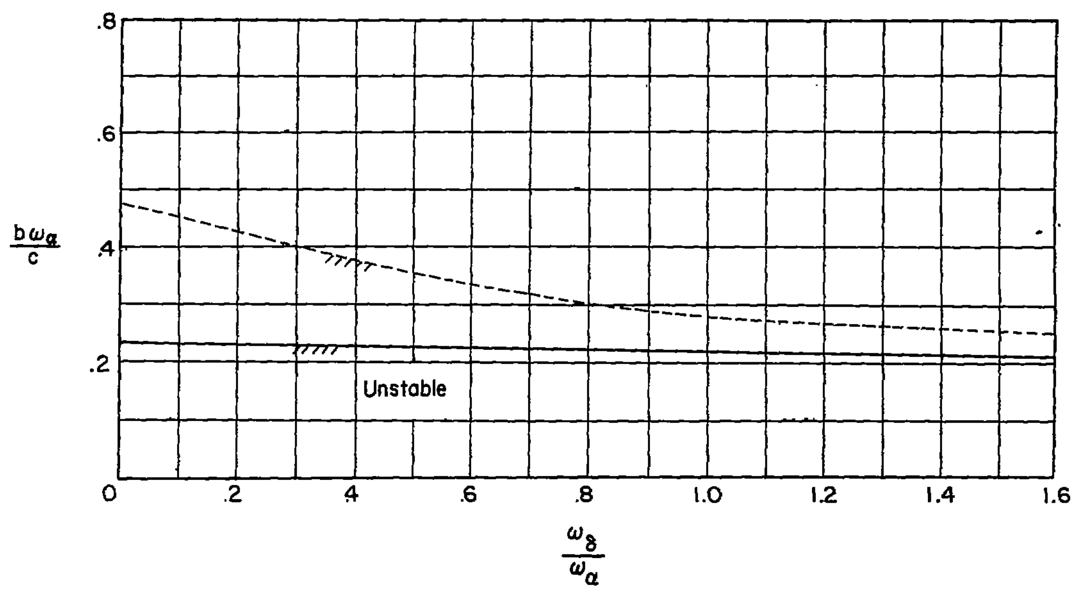

(b) Aileron at outboard location.

Figure 7.- Flutter parameter $b\omega_\alpha/c$ plotted against frequency ratio ω_δ/ω_h for wing-torsion—aileron rotation case employing finite-span theory. $M = 1.3$; $\frac{b\omega_\alpha}{c} = 2.08\,\frac{b\omega_h}{c}$; $\frac{\omega_\delta}{\omega_\alpha} = 0.480\,\frac{\omega_\delta}{\omega_h}$.